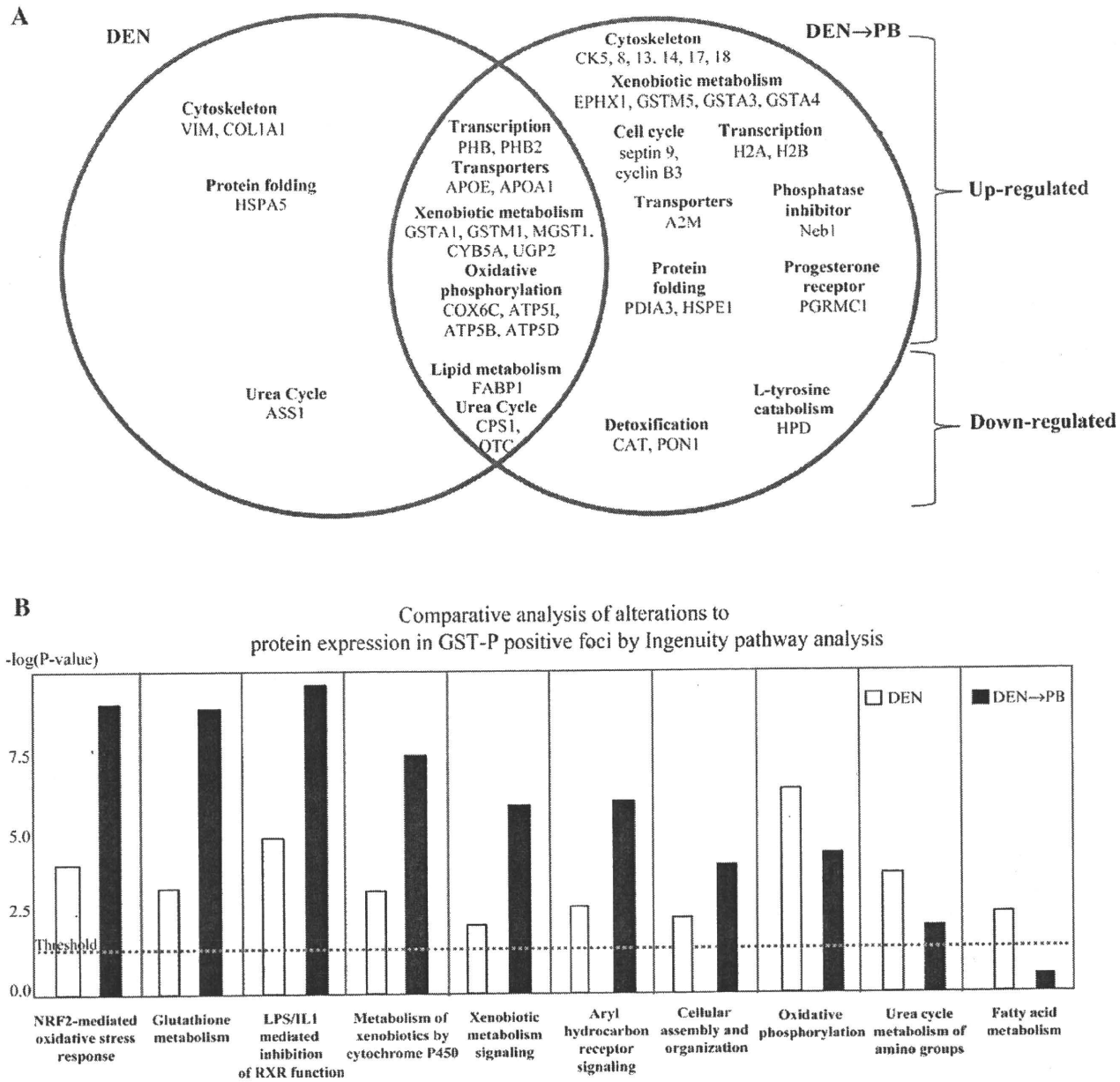

FIG. 1. Ingenuity pathway analysis for alterations to protein expression in liver GST-P$^+$ foci of rats treated with DEN followed by PB at a dose of 0 and 500 ppm for 10 weeks. (A) A Venn diagram comparing alterations to protein expression in GST-P$^+$ foci of rats treated with DEN alone and DEN followed by PB. (B) Comparative analysis of changes to canonical pathways in the GST-P$^+$ foci of rats in initiation control and promotion groups 13 weeks after DEN initiation. Numbers of proteins with altered expression are represented as ($-\log(p$ value)).

et al., 2010). It was further reported that an aberrant continuous activation of NRF2 in premalignant cells can promote cancer cell survival in response to an oxidizing tumor environment, which can be encountered by activation of oncogenic signals, altered metabolism, and mitochondrial dysfunction. Moreover, an important facet of NRF2 function is that it can cross-regulate the expression of factors controlling other signaling pathways, including the AhR and the NF-κB pathway (Kensler and Wakabayashi, 2010). On the other hand, AhR is known to interact with signaling pathways that are mediated by estrogen receptor and other hormone receptors, hypoxia, NF-κB, and to transactivate c-*myc* gene (Carlson and Perdew, 2002). Newly detected elevation of PHB and PHB2 in GST-P$^+$ foci as well as HCCs suggested the important role of these two proteins in onset of hepatocarcinogenesis. In line with our results, proteome analysis of the human HCC cell line, HCC-M,

Downloaded from toxsci.oxfordjournals.org at Osaka Shi U Rigakubu on January 3, 2011

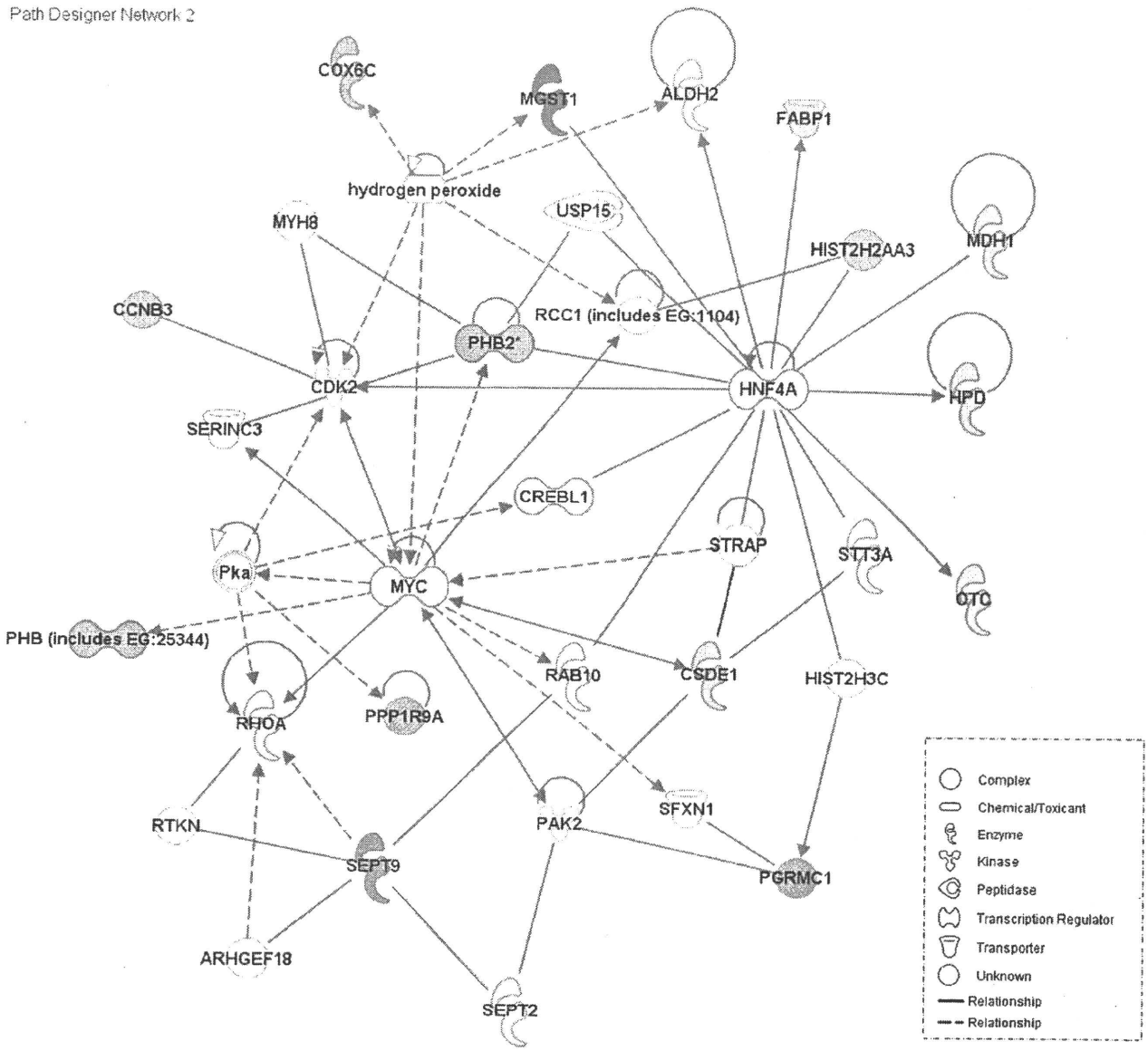

FIG. 2. Signaling pathway involving differentially expressed proteins in GST-P^{+} foci of rats treated with DEN followed by PB at a dose 500 ppm controlled by c-myc and HNF-4 transcriptional factors. Note overexpression (red) of PHB, PHB2, SEPT9, Neb1 (PPP1R9A), PGRMC1, histone H2aa3 (HIST2H2AA3) and downregulation (green) of OTC, HPD, and FAPB1.

revealed elevation of PHB (Seow *et al.*, 2000). It has been demonstrated that two PHB proteins, Phb1p and Phb2p, are located in the mitochondrial inner membrane where they form a large complex that represents a novel type of membrane-bound chaperone (Nijtmans *et al.*, 2002). The PHB complex binds directly to newly synthesized mitochondrial translation products and stabilizes them against degradation by membrane-bound metalloproteases belonging to the family of mitochondrial triple-A proteins. Human prohibitins have also been suggested to be localized in the nucleus and modulate transcriptional activity by interacting with various transcription factors, including nuclear receptors, either directly or indirectly (Tatsuta *et al.*, 2005). Recently, they have been demonstrated to be positive, rather than negative, regulators of cell proliferation in both plants and mice (Merkwirth *et al.*, 2008). Furthermore, PHB has been shown to colocalize with Rb in the nucleus, participating in transcriptional repression via N-CoR and HDAC1, inducing G1/S cell cycle arrest and associating with p53, thus, inhibiting apoptosis (Fusaro *et al.*, 2002). It has been further reported to interact with RING finger protein 2 (RNF2), a member of the PcG (polycomb group) family of proteins, and that the two proteins regulate the

Downloaded from toxsci.oxfordjournals.org at Osaka Shi U Rigakubu on January 3, 2011

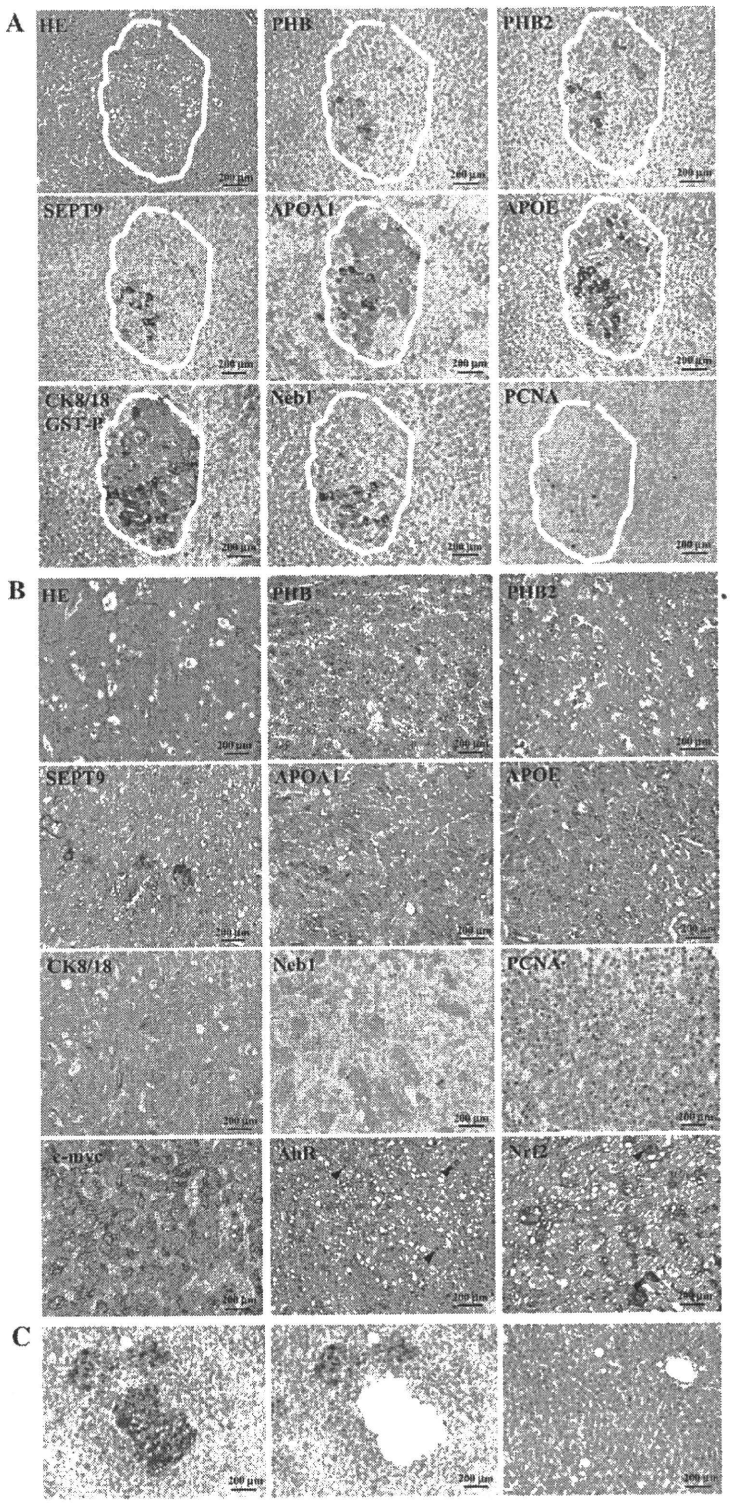

FIG. 3. Immunohistochemical analysis of PHB, PHB2, SEPT9, Neb1, CK8/18, APOE, APOA1, PCNA, c-myc, NRF2, and AhR in serial sections of rat livers after DEN initiation followed by PB at a dose of 500 ppm. GST-P (red) and CK8/18 (brown) positivity was demonstrated by double immunohistochemistry. (A) IHC analysis of protein expression in GST-P$^+$ foci of rats initiated with DEN followed by PB for 10 weeks. Note the coordinated staining pattern of overexpressed proteins in GST-P$^+$ foci. (B) IHC analysis of protein expression in HCCs of rats initiated with DEN followed by PB for 33 weeks. Arrows, overexpression of NRF2 and AhR in the nuclei of tumor cells in HCC. (C) Microdissected GST-P$^+$ foci and the photograph of the normal-appearing liver tissue of the rat initiated with DEN followed by PB for 10 weeks.

Downloaded from toxsci.oxfordjournals.org at Osaka Shi U Rigakubu on January 3, 2011

activity of E2F1 transcriptional factor via dual pathways: the direct, prohibitin-mediated pathway and the indirect, p16-mediated pathway of E2F1 transcriptional regulation (Choi *et al.*, 2008). PHB overexpression was shown to increase the expression of GST-P in intestinal cells and protect against oxidant-induced depletion of glutathione (Theiss *et al.*, 2007). In other studies, a striking correlation was revealed between mitochondrial targeting and the maintenance of cell proliferation, pointing to a crucial role of PHB2 within mitochondria (Tatsuta *et al.*, 2005). PHB2 is involved in recruitment of histone deacetylases, transcriptional repression by nuclear receptors, modulation of estrogen receptor transcriptional activity via NCOA1, mitochondrial respiration activity, and aging (Delage-Mourroux *et al.*, 2000). Furthermore, both prohibitins have been shown to be activated by c-*myc* and to have important roles in the control of apoptosis (O'Connell *et al.*, 2003).

Another protein regulating cell proliferation which was upregulated in GST-P$^+$ foci and HCCs is SEPT9. Highly expressed in neuronal tissues and breast cancer and a member of the cytoskeleton-related septin family, SEPT9, has been shown to be involved in cytokinesis, cell survival, and to suppress apoptosis (Roeseler *et al.*, 2009). Its altered expression has been implicated in neoplasia (Ito *et al.*, 2005). SEPT9 accelerated growth kinetics, stimulated cell motility, promoted invasion in Matrigel Transwell assays, increased genomic instability with the development of aneuploidy, and stimulated morphologic changes. Furthermore, there is growing evidence for cross talk between septin filaments and actin cytoskeleton (F-actin) which is regulated by Rho family of GTPases (Ito *et al.*, 2005). Moreover, SEPT9 methylated DNA has become recently used as a biomarker for colorectal cancer (Grutzmann *et al.*, 2008).

Interestingly, overexpression of another neuronal tissue protein Neb1 was detected in GST-P$^+$ foci of rats in the PB promotion group. A mosaic staining pattern for Neb1 was also observed in rat HCCs. Similar to SEPT9, this protein phosphatase 1-alpha inhibitor has been shown to bind to actin filaments (F-actin), show cross-linking activity and be involved in neurite and synapse formation and function (Nakanishi *et al.*, 1997). Furthermore, coexpression of neurabin with Lfc (lymphoid blast crisis's first cousin), a Rho guanine nucleotide exchange factor has been demonstrated to result in their clustering together with F-actin, a process that depended on Rho activity (Ryan *et al.*, 2005). Thus, both SEPT9 and Neb1 are likely to be involved in Rho-dependent organization of F-actin which might be a link between the microtubule, intermediate filaments, and F-actin cytoskeletons. Their role in liver preneoplasia needs further investigation.

The results of this study confirmed our recent demonstration of elevation of CK8 and CK18 expression in rat liver preneoplastic lesions leading to intermediate filament reorganization involving histone H2aa3 in the GST-P$^+$ foci of rats treated with DEN and PB (Kakehashi *et al.*, 2009). Moreover, overexpression of histone H2be was detected which might also play role in intermediate filament reorganization. Recently, CK8 and CK18 were reported to bind to the cytoplasmic domain of tumor necrosis factor receptor 2 (TNFR2) and moderate tumor necrosis factor (TNF) related to JNK intracellular signaling and NF-κB activation. This influence on TNF, a cytokine produced by macrophages and T lymphocytes affecting cellular proliferation, survival, differentiation, and cell death, may be the fundamental function of CK8 and CK18 common to liver regeneration and the reason for the persistent expression of these CKs in many carcinomas (Caulin *et al.*, 2000).

In the present experiment, cellular transporters APOA1, APOE, and A2M, secreted proteins detected in blood serum, plasma, and urine, were overexpressed in both GST-P$^+$ foci and HCCs. APOE and APOA1 are the proteins mediating binding, internalization, and catabolism of lipoprotein particles. APOE participates in Akt phosphorylation and can serve as a ligand for the low density lipoprotein (apo-B/E) receptor and for the specific apo-E receptor of hepatic tissues being overexpressed in response to reactive oxygen species (Fazio *et al.*, 2000). A2M, a cytokine transporter secreted in plasma, is able to inhibit all four classes of proteinases by a unique "trapping" mechanism (Sukata *et al.*, 2004). It has been reported to promote hepatocarcinogenesis by perturbing transforming growth factor-α–induced apoptosis. Elevation of A2M mRNA was detected in rat liver amphophilic cell foci induced by DEN and the peroxisomal proliferators Wy-14,643 or clofibrate (Sukata *et al.*, 2004).

An involvement of reactive oxygen species in the genesis of human cancers has been proposed, and a remarkable decrease of CAT mRNA levels and activity after immortalization and malignant transformation of mouse liver cells has been previously reported in line with our results (Sun *et al.*, 1993). The downregulation of CAT gene expression could be explained by a remarkable difference in methylation status of the CAT gene. Furthermore, CAT-negative hepatocytes did not show evidence of apoptosis or necrotic cell death (Oikawa and Novikoff, 1995). Similar to CAT, inhibition of PON1 was detected in both GST-P$^+$ foci and HCCs. PON1 is an arylesterase that mainly hydrolyzes the organophosphorus anticholinesterase compound paroxon to produce *p*-nitrophenol (Furlong, 2007). PON1 is also known to regulate lipid metabolic processes and be involved in responses to external stimuli, positively regulating cholesterol efflux and catabolism of aromatic compounds.

Urea cycle metabolic enzymes expression was here found suppressed in the GST-P$^+$ foci of both initiation control and PB-administered animals. These included CPS1, OTC, and ASS1 which are involved in the urea cycle of ureotelic animals where they play important roles in removing excess ammonia from the cell. In line with our results, its downregulation was previously observed in human HCCs (Chaerkady *et al.*, 2008).

In conclusion, early coordinated elevation of mitochondrial prohibitins and SEPT9 associated with induction of Neb1,

Downloaded from toxsci.oxfordjournals.org at Osaka Shi U Rigakubu on January 3, 2011

APOE, APOA1, A2M, PGRMC1, H2aa3, and CK5, CK8, CK13, CK14, CK17, and CK18, induction of cell proliferation, and suppression of detoxification system and urea cycle enzymes in areas of GST-P$^+$ foci suggested their involvement in onset and promotion of rat hepatocarcinogenesis leading to the development of HCCs. Combination of laser microdissection, QSTAR Elite LC-MS/MS, and iTRAQ technology thus might become a powerful tool for protein spectrum analysis, facilitating the search for mechanisms of carcinogenesis and identifying potential biomarkers for liver preneoplasia for early diagnosis.

FUNDING

Ministry of Health, Labor and Welfare of Japan [Grant-in-Aid for Scientific Research 19710167].

ACKNOWLEDGMENTS

We thank Masayo Inoue, Kaori Touma, and Rie Onodera for their technical assistance and Yukiko Iura for her help during preparation of this article.

REFERENCES

Caulin, C., Ware, C. F., Magin, T. M., and Oshima, R. G. (2000). Keratin-dependent, epithelial resistance to tumor necrosis factor-induced apoptosis. *J. Cell Biol.* **149,** 17–22.

Carlson, D. B., and Perdew, G. H. (2002). A dynamic role for the Ah receptor in cell signaling? Insights from a diverse group of Ah receptor interacting proteins. *J. Biochem. Mol. Toxicol.* **16,** 317–325.

Chaerkady, R., Harsha, H. C., Nalli, A., Gucek, M., Vivekanandan, P., Akhtar, J., Cole, R. N., Simmers, J., Schulick, R. D., Singh, S., *et al.* (2008). A quantitative proteomic approach for identification of potential biomarkers in hepatocellular carcinoma. *J. Proteome Res.* **7,** 4289–4298.

Choi, D., Lee, S. J., Hong, S., Kim, I. H., and Kang, S. (2008). Prohibitin interacts with RNF2 and regulates E2F1 function via dual pathways. *Oncogene* **27,** 1716–1725.

Delage-Mourroux, R., Martini, P. G., Choi, I., Kraichely, D. M., Hoeksema, J., and Katzenellenbogen, B. S. (2000). Analysis of estrogen receptor interaction with a repressor of estrogen receptor activity (REA) and the regulation of estrogen receptor transcriptional activity by REA. *J. Biol. Chem.* **275,** 35848–35856.

Fazio, S., Linton, M. F., and Swift, L. L. (2000). The cell biology and physiologic relevance of ApoE recycling. *Trends Cardiovasc. Med.* **10,** 23–30.

Furlong, C. E. (2007). Genetic variability in the cytochrome P450-paraoxonase 1 (PON1) pathway for detoxication of organophosphorus compounds. *J. Biochem. Mol. Toxicol.* **21,** 197–205.

Fusaro, G., Wang, S., and Chellappan, S. (2002). Differential regulation of Rb family proteins and prohibitin during camptothecin-induced apoptosis. *Oncogene* **21,** 4539–4548.

Gluckmann, M., Fella, K., Waidelich, D., Merkel, D., Kruft, V., Kramer, P. J., Walter, Y., Hellmann, J., Karas, M., and Kroger, M. (2007). Prevalidation of potential protein biomarkers in toxicology using iTRAQ reagent technology. *Proteomics* **7,** 1564–1574.

Grutzmann, R., Molnar, B., Pilarsky, C., Habermann, J. K., Schlag, P. M., Saeger, H. D., Miehlke, S., Stolz, T., Model, F., Roblick, U. J., *et al.* (2008). Sensitive detection of colorectal cancer in peripheral blood by septin 9 DNA methylation assay. *PLoS One* **3,** e3759.

Ito, H., Iwamoto, I., Morishita, R., Nozawa, Y., Narumiya, S., Asano, T., and Nagata, K. (2005). Possible role of Rho/Rhotekin signaling in mammalian septin organization. *Oncogene* **24,** 7064–7072.

Ito, N., Hasegawa, R., Imaida, K., Masui, T., Takahashi, S., and Shirai, T. (1992). Pathological markers for non-genotoxic agent-associated carcinogenesis. *Toxicol. Lett.* 64–65, Spec No. 613–620.

Kakehashi, A., Inoue, M., Wei, M., Fukushima, S., and Wanibuchi, H. (2009). Cytokeratin 8/18 overexpression and complex formation as an indicator of GST-P positive foci transformation into hepatocellular carcinomas. *Toxicol. Appl. Pharmacol.* **238,** 71–79.

Kakehashi, A., Kato, A., Inoue, M., Ishii, N., Okazaki, E., Wei, M., Tachibana, T., and Wanibuchi, H. (2010). Cytokeratin 8/18 as a new marker of mouse liver preneoplastic lesions. *Toxicol. Appl. Pharmacol.* **242,** 47–55.

Kensler, T. W., and Wakabayashi, N. (2010). Nrf2: friend or foe for chemoprevention? *Carcinogenesis* **31,** 90–99.

Kinoshita, A., Wanibuchi, H., Imaoka, S., Ogawa, M., Masuda, C., Morimura, K., Funae, Y., and Fukushima, S. (2002). Formation of 8-hydroxydeoxyguanosine and cell-cycle arrest in the rat liver via generation of oxidative stress by phenobarbital: association with expression profiles of p21(WAF1/Cip1), cyclin D1 and Ogg1. *Carcinogenesis* **23,** 341–349.

Kitano, M., Ichihara, T., Matsuda, T., Wanibuchi, H., Tamano, S., Hagiwara, A., Imaoka, S., Funae, Y., Shirai, T., and Fukushima, S. (1998). Presence of a threshold for promoting effects of phenobarbital on diethylnitrosamine-induced hepatic foci in the rat. *Carcinogenesis* **19,** 1475–1480.

Malhotra, D., Portales-Casamar, E., Singh, A., Srivastava, S., Arenillas, D., Happel, C., Shyr, C., Wakabayashi, N., Kensler, T. W., Wasserman, W. W., *et al.* (2010). Global mapping of binding sites for Nrf2 identifies novel targets in cell survival response through ChIP-Seq profiling and network analysis. *Nucleic Acids Res* **9,** 5718–5734.

Melle, C., Kaufmann, R., Hommann, M., Bleul, A., Driesch, D., Ernst, G., and von Eggeling, F. (2004). Proteomic profiling in microdissected hepatocellular carcinoma tissue using ProteinChip technology. *Int. J. Oncol.* **24,** 885–891.

Merkwirth, C., Dargazanli, S., Tatsuta, T., Geimer, S., Lower, B., Wunderlich, F. T., von Kleist-Retzow, J. C., Waisman, A., Westermann, B., and Langer, T. (2008). Prohibitins control cell proliferation and apoptosis by regulating OPA1-dependent cristae morphogenesis in mitochondria. *Genes Dev.* **22,** 476–488.

Nakanishi, H., Obaishi, H., Satoh, A., Wada, M., Mandai, K., Satoh, K., Nishioka, H., Matsuura, Y., Mizoguchi, A., and Takai, Y. (1997). Neurabin: a novel neural tissue-specific actin filament-binding protein involved in neurite formation. *J. Cell Biol.* **139,** 951–961.

Nijtmans, L. G., Artal, S. M., Grivell, L. A., and Coates, P. J. (2002). The mitochondrial PHB complex: roles in mitochondrial respiratory complex assembly, ageing and degenerative disease. *Cell Mol. Life Sci.* **59,** 143–155.

O'Connell, B. C., Cheung, A. F., Simkevich, C. P., Tam, W., Ren, X., Mateyak, M. K., and Sedivy, J. M. (2003). A large scale genetic analysis of c-Myc-regulated gene expression patterns. *J. Biol. Chem.* **278,** 12563–12573.

Oikawa, I., and Novikoff, P. M. (1995). Catalase-negative peroxisomes: transient appearance in rat hepatocytes during liver regeneration after partial hepatectomy. *Am. J. Pathol.* **146,** 673–687.

Roeseler, S., Sandrock, K., Bartsch, I., and Zieger, B. (2009). Septins, a novel group of GTP-binding proteins: relevance in hemostasis, neuropathology and oncogenesis. *Klin. Padiatr.* **221,** 150–155.

Ryan, X. P., Alldritt, J., Svenningsson, P., Allen, P. B., Wu, G. Y., Nairn, A. C., and Greengard, P. (2005). The Rho-specific GEF Lfc interacts with neurabin and spinophilin to regulate dendritic spine morphology. *Neuron* **47,** 85–100.

Downloaded from toxsci.oxfordjournals.org at Osaka Shi U Rigakubu on January 3, 2011

Seow, T. K., Ong, S. E., Liang, R. C., Ren, E. C., Chan, L., Ou, K., and Chung, M. C. (2000). Two-dimensional electrophoresis map of the human hepatocellular carcinoma cell line, HCC-M, and identification of the separated proteins by mass spectrometry. *Electrophoresis* **21,** 1787–1813.

Sukata, T., Uwagawa, S., Ozaki, K., Sumida, K., Kikuchi, K., Kushida, M., Saito, K., Morimura, K., Oeda, K., Okuno, Y., *et al.* (2004). Alpha(2)-macroglobulin: a novel cytochemical marker characterizing preneoplastic and neoplastic rat liver lesions negative for hitherto established cytochemical markers. *Am. J. Pathol.* **165,** 1479–1488.

Sun, Y., Colburn, N. H., and Oberley, L. W. (1993). Depression of catalase gene expression after immortalization and transformation of mouse liver cells. *Carcinogenesis* **14,** 1505–1510.

Tachibana, T., Okazaki, E., Yoshimi, T., Azuma, M., Kakehashi, A., and Wanibuchi, H. (2010). Rat monoclonal antibody specific for septin 9. *Hybridoma (Larchmt)* **29,** 169–171.

Tatsuta, T., Model, K., and Langer, T. (2005). Formation of membrane-bound ring complexes by prohibitins in mitochondria. *Mol. Biol. Cell* **16,** 248–259.

Theiss, A. L., Idell, R. D., Srinivasan, S., Klapproth, J. M., Jones, D. P., Merlin, D., and Sitaraman, S. V. (2007). Prohibitin protects against oxidative stress in intestinal epithelial cells. *FASEB J.* **21,** 197–206.

Wakabayashi, N., Slocum, S. L., Skoko, J. J., Shin, S., and Kensler, T. W. (2010). When NRF2 talks, who's listening? *Antioxid Redox Signal* **13,** 1649–1663.

Downloaded from toxsci.oxfordjournals.org at Osaka Shi U Rigakubu on January 3, 2011

Food and Chemical Toxicology 49 (2011) 471–476

Contents lists available at ScienceDirect

Food and Chemical Toxicology

journal homepage: www.elsevier.com/locate/foodchemtox

Non-genotoxic mode of action and possible threshold for hepatocarcinogenicity of Kojic acid in F344 rats

Yaowares Chusiri [a,b], Rawiwan Wongpoomchai [a,b], Anna Kakehashi [a], Min Wei [a], Hideki Wanibuchi [a], Usanee Vinitketkumnuan [b], Shoji Fukushima [c,*]

[a] Department of Pathology, Osaka City University Medical School, 1-4-3 Asahi-machi, Abeno-ku, Osaka 545-8585, Japan
[b] Department of Biochemistry, Faculty of Medicine, Chiang Mai University, 110 Intawaroros Road, Sutep, Muang, Chiang Mai 50200, Thailand
[c] Japan Bioassay Research Center, 2445 Hirasawa, Hadano, Kanagawa 257-0015, Japan

ARTICLE INFO

Article history:
Received 16 February 2009
Accepted 20 November 2010

Keywords:
Kojic acid
Hepatocarcinogenesis
Threshold
GST-P

ABSTRACT

Kojic acid (KA), a naturally occurring compound, is contained in traditional Japanese fermented foods and is used as a food additive, preservative and a dermatological skin-lightening agent. In the present experiment, initiation (experiment 1) and promotion (experiment 2) effects of KA-induced hepatocarcinogenesis were studied by rat medium-term bioassay for carcinogenicity. Male F344 rats were administered a diet containing 0–2% KA. Experiment 1 demonstrated that KA had no effect on induction of liver preneoplastic lesions or glutathione *S*-transferase placental form (GST-P) positive foci, in either number or area. In experiment 2, 2% KA treatment significantly increased the number and area of GST-P positive foci, but concentrations less than 0.5% did not. Moreover, 2% KA treatment significantly increased 8-OHdG levels and PCNA positive hepatocytes. The results indicated that low concentrations of KA do not have initiation effects on rat hepatocarcinogenesis, while higher concentrations of KA do promote hepatocarcinogenesis in rats. Thus, the results indicate that KA is a non-genotoxic hepatocarcinogen, showing the possible existence of a perfect threshold.

© 2010 Elsevier Ltd. All rights reserved.

1. Introduction

Chemical carcinogenesis, including hepatocarcinogenesis, has been classified into 'initiation' and 'promotion' stages. At present, promotion has further been subdivided into 'promotion' and 'progression'. Initiation involves mutation of hepatocellular DNA, thought to be irreversible and to consist of a single gene mutation that is caused by environmental genotoxic chemical agents, both physical and biological (e.g., viruses). Promotion follows initiation and involves aspects of gene activation, such as the latent phenotype of the initiated cell, which becomes expressed through cellular selection and clonal growth. This can proceed through a variety of mechanisms, including failure of apoptosis and failure to terminate proliferation of the initiated cell. Progression, the last stage, involves genetic damage that results in the conversion of benign tumors into malignant neoplasms capable of invading adjacent tissues and metastasizing to distant sites. The neoplastic progression may happen due to the errors in DNA replication and repairing DNA damage.

The various tests that have been used to identify carcinogenic agents may be classified into short, medium and long-term bioassays. Short-term assays have limited use, indirectly establishing an estimate of the risk that such chemicals pose for the human population. Long-term assays, for detection of carcinogenicity in experimental animals, have been the foundation for prediction of carcinogenic hazards to human beings. The standard requirements are – lifetime carcinogenicity testing in two rodent species, rats and mice, at three different doses of test compound with controls for each sex. This is, however, time-consuming and very expensive in terms of financial and human resources. Good animal facilities with experts in toxicology and toxicological pathology are essential for performance of the assays. Evaluating the performance of long-term bioassays, it became obvious that medium-term bioassays for carcinogenicity should be designed so as to reduce the time for the development of an endpoint. Carcinogens are generally classified into two categories: genotoxic and non-genotoxic. Genotoxic carcinogens have both initiation activity and promotion activity, and non-genotoxic carcinogens have promotion activity without initiation activity. Based on this concept, two-stage carcinogenic models as a medium-term carcinogenicity test have been developed for the detection of carcinogenicity in chemicals. Concerning the hepatocarcinogenicity of chemicals, medium-term carcinogenicity tests targeted for initiation activity or promotion activity have been established. The medium-term hepatocarcinogenesis bioassay of Ito et al. (1989, 2003), an 8-week experiment, utilizes

* Corresponding author. Tel.: +81 463 82 3911; fax: +81 463 82 3860.
E-mail address: s-fukushima@jisha.or.jp (S. Fukushima).

0278-6915/$ - see front matter © 2010 Elsevier Ltd. All rights reserved.
doi:10.1016/j.fct.2010.11.027

F344 rats that are given a single dose of diethylnitrosamine (DEN) to initiate carcinogenesis. After a 2-week period the rats are repeatedly exposed to a test compound for a dosing period of 6 weeks. At the end of week 3, rats are subjected to partial hepatectomy to maximize opportunities of promotion via a high rate of cell proliferation. All rats are sacrificed at the end of week 8 for evaluation of the development of preneoplastic hepatocellular foci by staining for expression of glutathione *S*-transferase placental form (GST-P) (Ito et al., 1989, 2003). Extensive testing has demonstrated that the induction of GST-P positive foci in the medium-term bioassay for liver carcinogens correlates well with the incidence of hepatocellular carcinomas in parallel long-term assays.

Genotoxic carcinogens are mutagenic and seem to act through interaction with DNA to produce irreversible genetic changes in target organ cells. It has been generally concluded that they have no dose threshold in their carcinogenic potential. Dose response assessment, to define relationships between doses of agents and the probability of induction of carcinogenic effect, is one of the most important components of risk assessment to humans. The dose–response relationship for genotoxic carcinogens is generally assumed to be linear without a threshold dose below which carcinogenic effects are absent. This means that genotoxic carcinogens may pose some risk at any level of exposure, although there is no definitive experimental evidence to support this suggestion. Several recently published papers attempt to find experimental evidence for the existence of a threshold in the dose–response for genotoxic carcinogens.

The different types of thresholds for carcinogens are opposed to the classical dose–response of carcinogens for which no threshold can be defined (Bolt et al., 2004). Hengstler et al. (2003) distinguished between perfect and practical thresholds, based on different types of mechanisms. Basically, non-genotoxic carcinogens have been connected with the perfect threshold. The carcinogens do not produce any DNA damage through inability of mode of action. A 'perfect threshold' has been attributed to mitotic spindle poisons where the primary interaction occurs with proteins and not with DNA. The definition of 'practical threshold' is based on the concept that the carcinogens should have no genotoxic effect at very low or immeasurable target concentrations. Such practical thresholds have been connected with rapid degradation (toxicokinetics) of the chemical or to factors in general that limit target exposures (Kirsch-Volders et al., 2000).

The human diet contains substantial amounts of a wide variety of natural mutagens and carcinogens. Kojic acid (KA; 5-hydroxy-2-(hydroxymethyl)-4H-pyran-4-one), a metabolic product of several species of *Aspergillus*, is contained in traditional Japanese fermented foods, including miso (soybean paste), soy sauce and sake, in levels up to 1 ppm (Burdock et al., 2001) and used as a food additive and preservative, and as a skin-whitening agent in cosmetics.

KA has an obscure toxicological profile. It was reported to be genotoxic in several *in vitro* tests, including mutation in *Salmonella typhimurium* strains TA98, TA100 and TA1535 either with or without metabolic activation, and the sister chromatid exchanges and chromosome aberrations test in Chinese hamster ovary (CHO) cells (Wei et al., 1991). However, all of the *in vivo* genotoxicity tests on KA were negative, including two independent mouse bone marrow micronucleus tests after a single administration and an unscheduled DNA synthesis test in rat hepatocytes (Nohynek et al., 2004).

It has been demonstrated that hepatocellular tumors were induced in B6C3F1 mice that were fed a diet containing 3% KA for 20 months (Fujimoto et al., 1998). In another study, it was reported that the incidence of hepatocellular adenomas as well as altered hepatocellular foci were increased in *p53*(+/−) and *p53*(+/+) mice fed 1.5% or 3% KA, as compared to those in untreated control mice (Takizawa et al., 2003). A recent report showed that a 20-week dietary administration of 2% KA with initiation treatment of *n*-bis(2-hydroxypropyl) nitrosamine (DHPN) increased the number and area of GST-P in the liver of F344 rats (Takizawa et al., 2004) and suggested possible hepatocarcinogenic potential of KA in the rat. Moreover, the initiating activities of KA on hepatocarcinogenesis have been investigated in F344 rats. The rats were given a single dose of KA followed by dietary administration of 0.015% 2-acetylaminofluorene (2-AAF) for 2 weeks and a single dose of CCl_4. The results suggest that KA has neither liver initiation activity nor capability of oxidative stress formation, but some evidence suggestive of liver tumor promoting effects in rats (Watanabe et al., 2005). The tumor-initiating activity of KA using partially hepatectomized mice was investigated, and the results suggest that KA has no tumor-initiating activity in mice livers (Moto et al., 2006). Thus there is a high possibility that KA has no *in vivo* genotoxic effects in rats.

In addition, KA has been reported to induce thyroid adenomas and hyperplasia formation in rodents, and the result was suggested to be due to its promoting activity (Fujimoto et al., 1998; Mitsumori et al., 1999; Tamura et al., 2001). Epidemiological studies show the occurrence of low incidence of thyroid cancer in the Japanese population (Marugame et al., 2006).

To confirm indistinct hepatocarcinogenicity of KA, a modified Tsuda's method (Tsuda et al., 1990, 1993; Takada et al., 1997) has been used for examination of initiation activity of rat hepatocarcinogenesis, and Ito's model (Ito et al., 1989, 2003) was used for examination of promotion activity.

2. Materials and methods

2.1. Chemicals

KA (CAS No. 501-30-4) (purity ⩾ 98%) and DEN were purchased from Tokyo Kasei Kogyo Co. Ltd. (Tokyo, Japan). KA was mixed into a powdered basal diet (CRF-1, Oriental Yeast Co. Ltd., Tokyo, Japan) at doses of 0.1%, 0.5% and 2% for experiment 1 (to examine initiation activity) and at doses of 0.001%, 0.01%, 0.1%, 0.5% and 2% for experiment 2 (to examine promotion activity). 2-AAF (CAS No. 53-96-3) was from Nacalai Tesque Inc., and mixed into powdered basal diet at a dose of 0.01%.

2.2. Animals

Five-week-old male F344 rats (60 rats in experiment 1 and 90 rats in experiment 2) were purchased from Charles River, Japan (Atsugi, Kanagawa, Japan). They were housed in an animal room, maintained on a 12 h (08:00–20:00) light/dark cycle at a constant temperature of 23 ± 1 °C and relative humidity of 44 ± 5% and were given free access to tap water and food. Animals were acclimated 1 week before the start of the experiment.

2.3. Experimental protocol

The scheme of the experiments is illustrated in Fig. 1. For detection of initiation activity of KA (experiment 1: liver initiation assay), 4 groups of 15 rats each were fed a diet containing 0, 0.1%, 0.5% or 2% KA for 4 weeks. Following an additional 2 weeks on a basal diet, rats were then fed a diet containing 0.01% 2-AAF for 2 weeks coupled with two-thirds partial hepatectomy during 2-AAF administration and continuation for an additional week's basal diet (Takada et al., 1997). The total observation period was 9 weeks.

For detection of the promotion activity of KA (experiment 2: liver promotion assay), the rats were divided into six groups (15 rats each). After 1 week on basal diet they underwent i.p. injection of DEN (200 mg/kg body wt.) dissolved in saline, to initiate

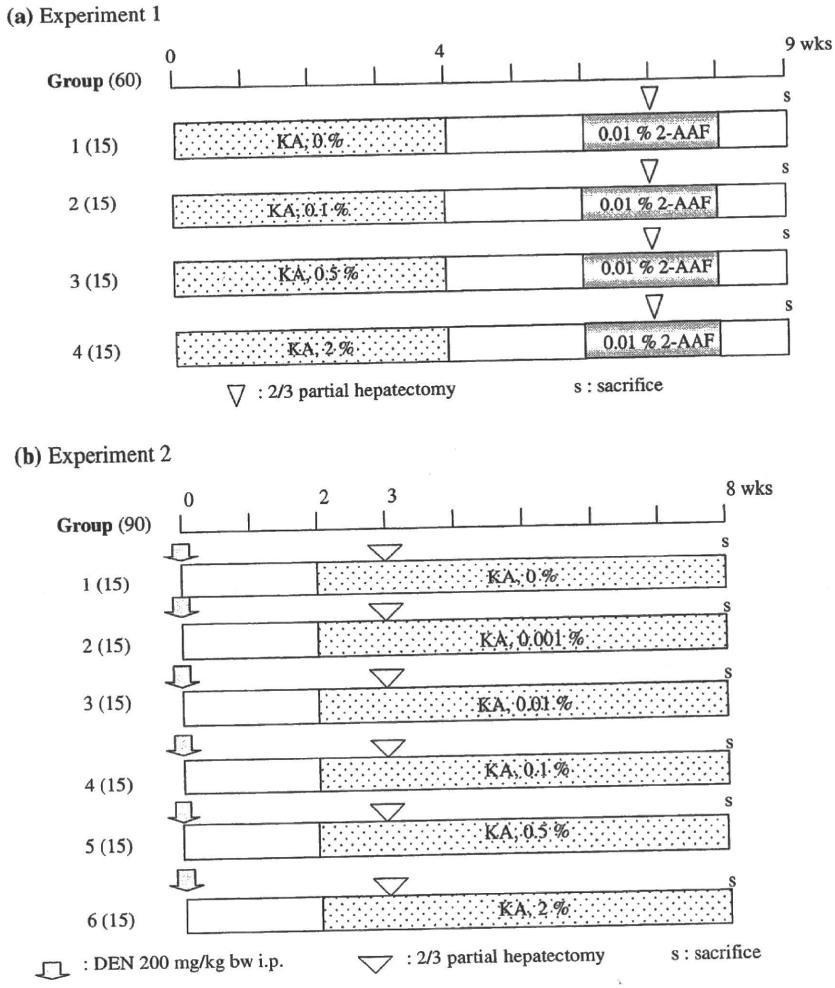

Fig. 1. Scheme of experimental designs.

hepatocarcinogenesis, and 2 weeks after that the rats were administered a diet containing KA 0%, 0.001%, 0.01%, 0.1%, 0.5% and 2% for 6 weeks. Animals were subjected to two-thirds partial hepatectomy at week 3 (Ito et al., 1989, 2003; Takada et al., 1994). The total observation period was 8 weeks.

All surviving animals were killed at the end of these experiments, their livers were removed and weighed, and then 2–3 mm thick sections from three lobes were fixed in formalin and embedded in paraffin wax. Sections cut at 4 μm were used for histopathological and immunohistochemical examination. The remaining liver tissue was preserved in liquid nitrogen.

These experiments were done under the guidelines of the animal facility of Osaka City University Medical School.

2.4. Immunohistochemistry for GST-P positive foci

The avidin–biotin peroxidase complex method (Vectastain ABC kit, Vector Lab.) was used to demonstrate the GST-P positive liver foci, a putative preneoplastic lesion. An immunohistochemical analysis was carried out with sequential treatments of rabbit anti-rat GST-P (1:2000) as a primary antibody, goat anti-rabbit IgG antibody as a secondary antibody, and the peroxidase-antiperoxidase complex. For final visualization of the GST-P positive foci, those that were larger than 0.2 mm in diameter were counted. The total area of liver sections was measured using an Image Processor for Analytical Pathology (IPAP; Sumica Technos, Osaka, Japan) to give values per cm^2 of liver section.

2.5. Immunohistochemistry for proliferation cell nuclear antigen (PCNA) and double immunohistochemistry for PCNA and GST-P

In experiment 1, PCNA staining was performed using an anti-PCNA mouse monoclonal antibody (1:500). After deparaffinizing with xylene, alcohol and distilled water, endogenous peroxidase was blocked with 3% hydrogen peroxide (H_2O_2) for 5 min. The sections were then treated in a microwave oven in a solution of 0.1 mM citrate buffer pH 6.0 for 15 min and then transferred to distilled water. After rinsing in phosphate buffer saline (PBS), the sections were incubated with normal horse serum in PBS for 15 min. For detection of PCNA, the sections were incubated with anti-PCNA mouse monoclonal antibody at 37 °C for 1 h and then incubated with anti-mouse IgG antibody as a secondary antibody for 30 min at room temperature. Color was developed with diaminobenzidine tetrachloride (DAB). Finally, the sections were counterstained with haematoxylin, dehydrated and placed on a cover slide. The PCNA indices were counted as the number of positive nuclei per 1000 hepatocytes.

In experiment 2, double staining for PCNA and GST-P positive foci was performed using the same method as described before. After developing color with DAB, the sections were washed in running tap water and Tris–HCl–phosphate buffer saline (TBS). For GST-P detection, the sections were blocked for unspecific binding with normal goat serum in TBS for 15 min and then incubated with rabbit anti-rat GST-P antibody at 1:2000 dilutions as the primary antibody at 37 °C for 1 h. After that, the sections were incubated

Table 1
Final body weight, liver weights and food and water consumption of rats treated with various concentrations of KA (experiment 1).

Treatment	No. of rat examined	Final body weight (g)	Food consumption (g/rat/day)	Water consumption (g/rat/day)	Liver weight	
					Absolute (g)	Relative (%)
0% KA	15	249.7 ± 10.1	13.0 ± 3.8	18.2 ± 3.3	5.76 ± 0.73	2.31 ± 0.29
0.1% KA	15	265.7 ± 11.5*	13.5 ± 3.9	18.7 ± 3.6	6.66 ± 0.79*	2.51 ± 0.29
0.5% KA	14	267.8 ± 10.6*	13.2 ± 3.1	18.7 ± 3.4	6.73 ± 1.40*	2.50 ± 0.47
2% KA	15	247.1 ± 11.1	11.1 ± 2.7	16.7 ± 2.5	6.12 ± 0.49	2.48 ± 0.17

* Significantly different from control group (DEN alone) at $p < 0.05$.

with DAKO Envision labelled polymer-AP (mouse/rabbit) for 30 min and color developed with DAKO New Fuchin Substrate System. Finally, the sections were counterstained with haematoxylin and mounted with Aquatex. The PCNA indices were estimated for GST-P positive areas as numbers of positive nuclei per 1000 cells.

2.6. Measurement of 8-OHdG levels in DNA

DNA samples were isolated from pieces of frozen liver weighing 500 mg using DNA Extractor WB kit (Wako Pure Chemical Industries Ltd., Osaka, Japan), containing sodium iodide (NaI), deferoxamine mesylate (Sigma Chemical Co., St. Louis, MO) and RNase (Wako Pure Chemical Industries Ltd., Osaka, Japan), then digested into deoxynucleosides by combined treatment with nuclease P1 and alkaline phosphatase. Finally the samples were filtered using an Ultrafree-MC 100,000NMWL filter unit (Millipore Co., Bedford, MA). The level of 8-OHdG in each resultant preparation was determined by HPLC-ECD using a Beckman Coulter Ultrasphere Ods column 4.6 mm × 25 cm which controlled the temperature at 35 °C, flow rate 1 ml/min, L2D2 lamp and Esa Coulochem II electrochemical detector. The level of 8-OHdG formation was expressed as the number of 8-OHdG residues/10^5 total deoxyguanosines.

2.7. Immunohistochemistry for apoptosis

Immunohistochemistry for apoptosis (TUNEL) were performed using an ApopTag Peroxidase *in situ* kit (Chemicon International Inc., Germany). After deparaffinization, the sections were pretreated with proteinase K (20 μg/ml) and endogenous peroxidase quenched with 3% H_2O_2. Then, the sections were enzymatically added to terminal deoxynucleotidyl transferase (TdT) and labeled with the digoxigenin-nucleotide. After that, they were allowed to bind with an anti-digoxigenin antibody that was conjugated to a peroxidase reporter molecule. Finally, the bound peroxidase antibody was conjugated enzymatically and generated color from a chromogenic substrate. The apoptotic index is assessed as apoptotic bodies per 1000 hepatocytes.

2.8. Statistical analysis

All results are presented as mean ± SD. All of the statistical analyses were carried out by Dunnett's multiple comparison tests. Statistical significance was evaluated at $p < 0.05$.

3. Results

3.1. Experiment 1: liver initiation assay

Final body weight and absolute liver weights were significantly increased in the group administered the KA at concentrations of 0.1% and 0.5% as compared with the values for the control groups, but there were no significant differences among the groups with regard to food and water consumption (Table 1). No change in liver/body weight ratio was induced by the administration of KA at various concentrations as compared with the control group. The food and water intake of the 2% KA fed group were slightly less than those of the other groups due to the KA treatment. Rat's appetite became normal after cessation of KA feeding.

Table 2
GST-P positive foci and 8-OHdG level of rats treated with various concentrations of KA (experiment 1) (diameter ⩾ 0.2 mm) (mean ± SD).

Treatment	No. of rat examined	GST-P positive foci		8-OHdG level (8-OHdG/10^5 dG)
		Number (No./cm^2)	Area (mm^2/cm^2)	
0% KA	15	2.67 ± 1.07	0.15 ± 0.08	0.16 ± 0.02
0.1% KA	15	2.13 ± 0.47	0.13 ± 0.07	0.14 ± 0.01
0.5% KA	14	2.84 ± 0.77	0.16 ± 0.09	0.17 ± 0.04
2% KA	15	3.69 ± 1.53	0.18 ± 0.09	0.20 ± 0.05

Data on the effect of various concentrations of KA on formation of GST-P positive foci in the liver are shown in Table 2. Two percent KA slightly increased GST-P positive foci in the number ($p = 0.074$) and area ($p = 0.554$) of GST-P positive foci formation compared with non-treated groups, but there was no significant difference. Furthermore, there were no remarkable differences between KA-treated and non-treated groups in 8-OHdG formation levels in rat liver DNA (Table 2). PCNA positive index and apoptotic index did not change among groups (data not shown).

3.2. Experiment 2: liver promotion assay

Data on the effect of KA application at different concentrations by body weight and liver weight after DEN-initiation are shown in Table 3. There were no significant differences among the groups with regards to food and water consumption. After 6 weeks of continuous KA administration to rats initiated with DEN, the 2% KA treatment significantly increased absolute and relative liver weights but slightly decreased final rat body weight (Table 3).

In 2% KA-treated rats, the numbers and areas of GST-P positive foci were markedly increased, while 0.001–0.5% KA treatment had no effect on GST-P positive foci formation compared with a control group (Fig. 2). Histological examination found that high concentration of KA induced centrilobular hypertrophy, eosinophilic focus, basophilic focus and mixed cell focus, which were all correlated with GST-P positive foci in rat livers. The 2% KA-treated group also showed a significantly increased PCNA positive index in the GST-P area (Table 4). HPLC analysis revealed 8-OHdG levels in rat livers to be significantly increased in the group fed with 0.5% and 2% KA. Analysis via the TUNEL assay demonstrated significant increases of apoptosis in the livers of rats treated with 0.01% and 0.1% KA, but not in those treated with 0.5% and 2% after DEN initiation.

4. Discussion

In the present study, we examined the initiation activity of KA in a medium-term liver initiation assay using partially hepatectomized rats. The many indicators assessed, including GST-P positive foci, widely recognized to be hepatocellular preneoplastic lesions,

Table 3
Final body weight, liver weights and food and water consumption of rats treated with various concentrations of KA after DEN-initiation (experiment 2).

Treatment	No. of rats examined	Body weight (g)	Food consumption (g/rat/day)	Water consumption (g/rat/day)	Liver weight	
					Absolute (g)	Relative (%)
DEN	15	240.4 ± 15.0	12.4 ± 2.6	18.2 ± 1.7	7.06 ± 0.38	2.97 ± 0.12
DEN + 0.001% KA	13	250.4 ± 6.3	12.4 ± 3.1	18.4 ± 2.2	7.40 ± 0.38	2.96 ± 0.13
DEN + 0.01% KA	15	251.7 ± 14.7	12.2 ± 2.6	18.7 ± 1.6	7.19 ± 0.47	2.85 ± 0.14
DEN + 0.1% KA	15	254.5 ± 8.6	12.2 ± 2.7	18.2 ± 1.7	6.68 ± 0.95	2.67 ± 0.18
DEN + 0.5% KA	15	246.5 ± 7.6	12.2 ± 3.1	17.8 ± 2.1	7.58 ± 0.41	3.02 ± 0.08
DEN + 2% KA	14	227.5 ± 8.9	11.1 ± 2.5	16.8 ± 2.0	7.90 ± 0.49*	3.46 ± 0.21*

* Significantly different from control group (DEN alone) at $p < 0.05$.

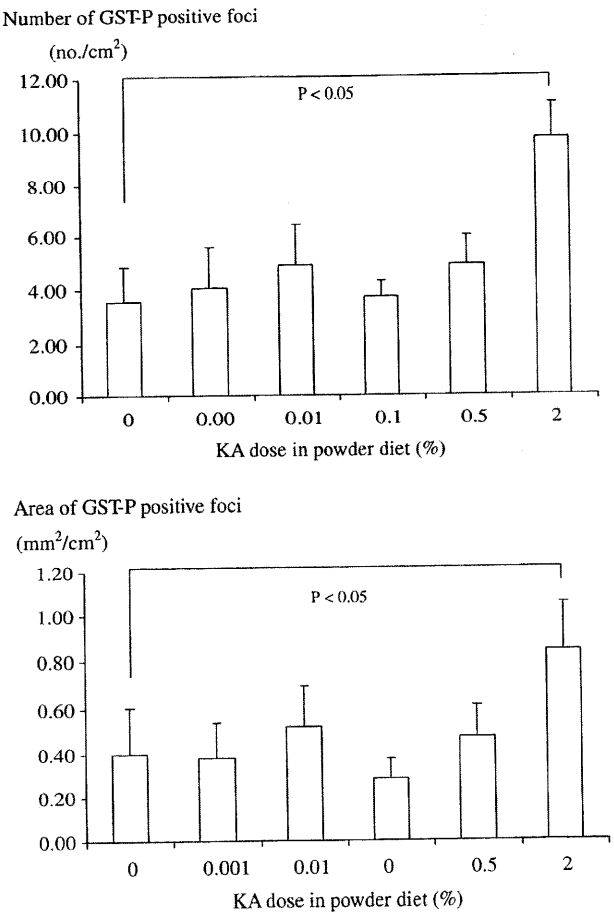

Fig. 2. Number and area of GST-P positive liver cell foci in partially hepatectomized rat treated with various concentrations of KA after DEN initiation (Experiment 2). Data represent the mean ± SD.

8-OHdG formation, cell proliferation and apoptotic index, were not significantly different in the groups treated with various concentrations of KA compared to the control groups. Although there were body weight changes during the experiment, these results showed no relation with the other carcinogenesis biomarkers. Even though there were body weight decreases in the 2% KA-treated group during the KA treatment period, these returned to normal in the final stages after cessation of KA feeding. The same results were observed by Higa et al. (2007). On the other hand, the body weight of low concentrations of KA treated rats significantly increased. This may be partly due to the influence of KA on thyroid hormones which regulate rat basal metabolism (Fujimoto et al., 1999; Bray et al., 1976). From previous studies, it is still unclear whether KA is a genotoxic or non-genotoxic carcinogen. The genotoxic profile of KA has been reported as positive in (1) Ames assay either with or without metabolic activation at high concentration of KA; (2) sister chromatid exchange and chromosome aberration in CHO cells (Wei et al., 1991); and (3) induced thyroid-proliferative lesions in rodents (Fujimoto et al., 1998; Mitsumori et al., 1999; Moto et al., 2006). These studies contradict the negative results from rat hepatocyte unscheduled DNA synthesis and bone marrow micronucleus tests (Nohynek et al., 2004), and lack of initiating activity on rodent hepatocarcinogenesis (Watanabe et al., 2005; Moto et al., 2006). In our study for initiation activity, the induction of GST-P positive foci in the rat livers did not show any significant difference. In addition, 8-OHdG formation level was also found not to differ from that of the control group. Therefore, we conclude that KA does not have any initiation activity on rat hepatocarcinogenesis.

To investigate the promoting activity on rat hepatocarcinogenesis, DEN was used as an initiator following administering to rats of various concentrations of KA in the diet, and in parallel with partial hepatectomy. The data demonstrated that only high concentration (2%) of KA significantly induced the number and area of GST-P positive foci formation. These results agree with those of Takizawa and his colleagues (Takizawa et al., 2004). Furthermore, our studies suggest that the low concentration (0.001%) of KA in the daily intake of humans should have no adverse effects. Moreover, the experiment showed no effect on GST-P positive foci formation at low and medium concentrations (0.01–0.5 %). 8-OHdG formation levels significantly increased with KA at concentrations of 0.5% and 2%, and cell proliferation was significantly increased at a concentration of 2%. Thus, KA increasing GST-P formation with a high concentration of KA might be involved with oxidative stress induc-

Table 4
PCNA positive index, 8-OHdG level and apoptotic index of rats treated with various concentrations of KA after DEN-initiation (experiment 2).

Treatment	No. of rats examined	PCNA positive index (No./1000 hepatocyte)	8-OHdG level (per 10^5 dG)	Apoptotic index (No./1000 hepatocyte)
DEN	15	19.68 ± 1.87	0.37 ± 0.07	14.00 ± 1.86
DEN + 0.001% KA	13	17.49 ± 0.54	0.46 ± 0.06	11.91 ± 1.58
DEN + 0.01% KA	15	16.99 ± 3.45	0.41 ± 0.08	20.56 ± 4.71*
DEN + 0.1% KA	15	16.44 ± 2.92	0.39 ± 0.06	26.57 ± 4.60*
DEN + 0.5% KA	15	20.96 ± 1.33	0.58 ± 0.08*	14.20 ± 2.34
DEN + 2% KA	14	24.10 ± 1.46*	0.57 ± 0.04*	12.88 ± 3.19

* Significantly different from control group (DEN alone) at $p < 0.05$.

tion and increased cell proliferation, while there are no effects on apoptotic pathways. These findings may indicate that KA exerts a promoting activity of rat hepatocarcinogenesis at high concentration, but not at low, showing the existence of a threshold in KA carcinogenicity. This corresponds to the observations of Umemura et al. (1999) that pentachlorophenol (PCP) induces promotion but does not initiate heaptocarcinogenesis in B6C3F1 mice livers.

In another study we examined the effect of KA on xenobiotic metabolizing enzyme (P450) via a short term study. Briefly, rats were given KA by oral administration at various concentrations for 2 weeks and then the livers were analyzed for hepatic P450 levels in various isozymes using Western blot analysis. Doses of 2% KA significantly increased CYP2B1 level (unpublished data). Klaunig and Kamendulis (2004) proposed that reactive oxygen species (ROS), such as superoxide anions, or hydrogen peroxide and hydroxyl radicals, can be produced from several sources during metabolism by cytochrome P450. Similarly, metabolism of Phenobarbital by CYP2B is involved in the oxygenation and uncoupling of catalytic activation and subsequent release of superoxide anions. In addition, the ROS can react with DNA to form oxidative DNA damage, 8-OHdG – which is a marker of cellular oxidative stress during carcinogenesis (Kasai, 1997). Thus, KA treatment at high doses in the promotion stage induced overexpression of P450, such as CYP2B1. This may contribute to an increase of 8-OHdG formation through ROS, which then promotes an increase of cell proliferation and finally increases induction of GST-P positive foci. Thus, the induction of oxidative stress has an important role for KA hepatocarcinogenesis in rats. Biochemical processes are capable of repairing the DNA damage. Since, in experiment 1, liver samples measured for 8-OHdG formation were obtained 5 weeks after cessation of KA treatment, the formation levels would not be different among the various groups.

KA carcinogenicity in rat livers has a non-genotoxic mode of action; we observed no initiation activity but did find positive promotion activity. Moreover, since the promotion activity was exerted only at high concentration (2% KA), the carcinogenic effect of KA will not occur up to a certain defined threshold dose level. A gradual dose–response may be defined to correlate dose level with 8-OHdG formation in GST-P positive foci and GST-P positive foci induction. Previous mechanistic studies aimed to explain the carcinogenic activity of non-genotoxic carcinogens have shown that the carcinogenic effect only occurs when high doses are used in order to produce prolonged interference with physiological control and modifications of cellular proliferation patterns (Purchase, 1994). Therefore, a perfect threshold of KA may exist for hepatocarcinogenicity in rats.

In conclusion, KA has no initiation activity on rat hepatocarcinogenesis, while high concentrations exert promotion activity, showing the possible existence of a threshold for rat hepatocarcinogenicity.

Conflicts of Interest

The authors declare that there are no conflicts of interest.

Acknowledgements

The authors would like to thank Kang Jin Seok for pathological morphology suggestion and Kaori Touma, Masayo Inoue and Rie Onodera for technical support.

References

Bolt, H.M., Foth, H., Hengstler, J.G., Degen, G.H., 2004. Carcinogenicity categorization of chemicals – new aspects to be considered in a European perspective. Toxicol. Lett. 151, 29–41.

Bray, G.A., Fisher, D.A., Chopra, I.J., 1976. Relation of thyroid hormones to bodyweight. Lancet 307 (7971), 1206–1208.

Burdock, G.A., Soni, M.G., Carabin, I.G., 2001. Evaluation of health aspects of kojic acid in food. Regul. Toxicol. Pharmacol. 33, 80–101.

Fujimoto, N., Watanabe, H., Nakatani, T., Roy, G., Ito, A., 1998. Induction of thyroid tumors in (C57BL/6N X C3H/N)F1 mice by oral administration of kojic acid. Food Chem. Toxicol. 36, 697–703.

Fujimoto, N., Onodera, H., Mitsumori, K., Tamura, T., Maruyama, S., Ito, A., 1999. Changes in thyroid function during development of thyroid hyperplasia induced by kojic acid in F344 rats. Carcinogenesis 20 (8), 1567–1571.

Hengstler, J.G., Bogdanffy, M.S., Bolt, H.M., Oesch, F., 2003. Challenging dogma: thresholds for genotoxic carcinogens? The case of vinyl acetate. Annu. Rev. Pharmacol. Toxicol. 43, 485–520.

Higa, Y., Kawabe, M., Nabae, K., Toda, Y., Kitamoto, S., Hara, T., Tanaka, N., Kariya, K., Takahashi, M., 2007. Kojic acid – absence of tumor-initiating activity in rat liver, and of carcinogenic and photo-genotoxic potential in mouse skin. J. Toxicol. Sci. 32 (2), 143–159.

Ito, N., Tamano, S., Shirai, T., 2003. A medium-term rat liver bioassay for rapid *in vivo* detection of carcinogenic potential of chemicals. Cancer Sci. 94 (1), 3–8.

Ito, N., Tatematsu, M., Hasegawa, R., Tsuda, H., 1989. Medium-term bioassay system for detection of carcinogens and modifiers of hepatocarcinogenesis utilizing the GST-P positive liver cell focus as an endpoint marker. Toxicol. Pathol. 17 (4), 630–641.

Kasai, H., 1997. Analysis of a form of oxidative DNA damage, 8-hydroxy-2′-deoxyguanosine, as a marker of cellular oxidative stress during carcinogenesis. Mutat. Res. 387, 147–163.

Kirsch-Volders, M., Aardema, M., Elhajouji, A., 2000. Concepts of threshold in mutagenesis and carcinogenesis. Mutat. Res. 464, 3–11.

Klaunig, J.E., Kamendulis, L.M., 2004. The role of oxidative stress in carcinogenesis. Annu. Rev. Pharmacol. Toxicol. 44, 239–267.

Mitsumori, K., Onodera, H., Takahashi, M., Funakoshi, T., Tamura, T., Yasuhara, T., Takegawa, K., Takahashi, M., 1999. Promoting effects of kojic acid due to serum TSH elevation resulting from reduced serum thyroid hormone levels on development of thyroid proliferative lesions in rats initiated with N-*bis*(2-hydroxypropyl)nitrosamine. Carcinogenesis 20, 173–176.

Moto, M., Mori, T., Okamura, M., Kashida, Y., Mitsumori, K., 2006. Absence of liver tumor-initiating activity of kojic acid in mice. Arch. Toxicol. 80 (5), 299–304.

Marugame, T., Kamo, K., Katanoda, K., Ajiki, W., Sobue, T., 2006. Cancer incidence and incidence rates in Japan in 2000: Estimates based on data from 11 population-based cancer registries. Jpn. J. Clin. Oncol. 36 (10), 668–675.

Nohynek, J.G., Kirkland, D., Marzin, D., Toutain, H., Leclerc-Ribaud, C., Jinnai, H., 2004. An assessment of genotoxicity and human health risk of tropical use of kojic acid [5-hydroxy-2-(hydroxymethyl)-4H-pyran-4-one]. Food Chem. Toxicol. 42, 93–105.

Purchase, I.F.H., 1994. Current knowledge of mechanisms of carcinogenicity: genotoxins versus non-genotoxins. Hum. Exp. Toxicol. 13, 17–28.

Takada, N., Matsuda, T., Otoshi, T., Yano, Y., Otani, S., Hasegawa, T., Nakae, D., Konishi, Y., Fukushima, S., 1994. Enhancement by organosulfur compounds from garlic and onions of diethylnitrosamine-induced glutathione S-transferase positive foci in the rat liver. Cancer Res. 54 (11), 2895–2899.

Takada, N., Yano, Y., Wanibushi, H., Otani, S., Fukushima, S., 1997. S-methylcysteine and cysteine are inhibitors of induction of glutathione S-transferase placental form-positive foci during initiation and promotion phases of rat hepatocarcinogenesis. Jpn. J. Cancer Res. 88 (5), 435–442.

Takizawa, T., Imai, T., Onose, J., Ueda, M., Tamura, T., Mitsumori, K., Izumi, K., Hirose, M., 2004. Enhancement of hepatocarcinogenesis by kojic acid in rat two-stage models after initiation with N-*bis*(2-hydroxypropyl)nitrosamine or N-diethylnitrosamine. Toxicol. Sci. 81, 43–49.

Takizawa, T., Mitsumori, K., Tamura, T., Nasu, M., Ueda, M., Imai, T., Hirose, M., 2003. Hepatocellular tumor induction in heterozygous *p53*-deficient CBA mice by a 26-week dietary administration of kojic acid. Toxicol. Sci. 73, 287–293.

Tamura, T., Mitsumori, K., Onodera, H., Fujimoto, N., Yasuhara, K., Takegawa, K., Takagi, H., Hirose, M., 2001. Dose-threshold for thyroid tumor-promoting effects of orally administered kojic acid in rats after initiation with *N-bis*(2-hydroxypropyl)nitrosamine. J. Toxicol. Sci. 26 (2), 85–94.

Tsuda, H., Matsumoto, K., Ogino, H., Ito, M., Hirono, I., Nagao, M., Sato, K., Cabral, R., Bartsch, H., 1993. Demonstration of initiation potential of carcinogens by induction of preneoplastic glutathione S-transferase P-form-positive liver cell foci: possible *in vivo* assay system for environmental carcinogens. Jpn. J. Cancer Res. 84 (3), 230–236.

Tsuda, H., Takahashi, S., Yamaguchi, S., Ozaki, K., Ito, N., 1990. Comparison of initiation potential of 2-amino-3-methylimidazo[4,5-f]quinoline and 2-amino-3,8-dimethylimidazo[4,5-f]quinoxaline in an *in vivo* carcinogen bioassay system. Carcinogenesis 11 (4), 549–552.

Umemura, T., Kai, S., Hasegawa, R., Sai, K., Kurokawa, Y., Williams, G.M., 1999. Pentachlorophenol (PCP) produces liver oxidative stress and promotes but does not initiate hepatocarcinogenesis in B6C3F1 mice. Carcinogenesis 20 (6), 1115–1120.

Watanabe, T., Mori, T., Kitamura, Y., Umemura, T., Okamura, M., Kashida, Y., Nishikawa, A., Hirose, M., Mitsumori, K., 2005. Lack of initiating activity of kojic acid on hepatocarcinogenesis in F344 rats. J. Toxicol. Pathol. 18, 79–84.

Wei, C.I., Huang, T.S., Fernando, S.Y., Chung, K.T., 1991. Mutagenicity studies of kojic acid. Toxicol. Lett. 59, 213–220.

Tumor-associated MUC5AC stimulates *in vivo* tumorigenicity of human pancreatic cancer

HIROTAKA HOSHI[1,3], TETSUJI SAWADA[2], MOTOYUKI UCHIDA[1], HIKARU SAITO[1], HIROKO IIJIMA[1], MIKAKO TODA-AGETSUMA[1], TSUTOMU WADA[1], SADAAKI YAMAZOE[2], HIROAKI TANAKA[2], KENJIRO KIMURA[2], ANNA KAKEHASHI[3], MIN WEI[3], KOSEI HIRAKAWA[2] and HIDEKI WANIBUCHI[3]

[1]Biomedical Research Laboratories, Kureha Corporation, 3-26-2 Hyakunin-cho, Shinjuku-ku, Tokyo 169-8503; Departments of [2]Surgical Oncology and [3]Pathology, Osaka City University Graduate School of Medicine, 1-4-3 Asahi-machi, Abeno-ku, Osaka 545-8585, Japan

Received September 30, 2010; Accepted November 8, 2010

DOI: 10.3892/ijo.2011.911

Abstract. MUC5AC, a high molecular weight glycoprotein, is overexpressed in the ductal region of human pancreatic cancer but is not detectable in the normal pancreas, suggesting its association with disease development. In the present study, we investigated the *in vitro* and *in vivo* effects of MUC5AC knockdown by short interfering RNA (siRNA) in the MUC5AC-overexpressing SW1990 and BxPC3 human pancreatic cancer cell lines in order to clarify its function. Significant decreases in the expression levels of MUC5AC mRNA and protein were observed in SW1990 and BxPC3 cells that had been stably transfected with a MUC5AC siRNA expression vector (SW1990/si-MUC5AC and BxPC3/si-MUC5AC cells) compared to those in cells transfected with an si-mock vector (SW1990/si-mock and BxPC3/si-mock cells). In *in vitro* studies, neither type of MUC5AC-knockdown cell showed any difference in cell survival, proliferation, or morphology from the si-mock cells or parental cells. However, *in vivo* xenograft studies demonstrated that MUC5AC knockdown significantly reduced the tumorigenicity and suppressed the tumor growth of si-MUC5AC cells compared to those of the si-mock cells. Immunohistochemical analysis revealed that CD45R/B220$^+$ and Gr-1$^+$ cells had infiltrated into the tumor tissue of the SW1990/si-MUC5AC cells. Furthermore, cancer-associated antigen specific antibodies were detected at high levels in the sera from the SW1990/si-MUC5AC cell-bearing mice. These results suggest that tumor-associated MUC5AC expressed on the surface of pancreatic cancer cells supports the escape of pancreatic cancer cells from immunosurveillance. The present findings highlight a new dimension of MUC5AC as a functional immunosuppressive agent and its important role in pancreatic cancer progression.

Correspondence to: Dr Tetsuji Sawada, Department of Surgical Oncology, Osaka City University Graduate School of Medicine, 1-4-3 Asahi-machi, Abeno-ku, Osaka 545-8585, Japan
E-mail: m1355299@med.osaka-cu.ac.jp

Key words: MUC5AC, mucin, glycoprotein, immunosuppression, short interfering RNA (siRNA), pancreatic cancer

Introduction

Mucins are heavily glycosylated proteins that are expressed in mucosal tissues, establish a selective molecular barrier at the epithelial surface, and engage in signal transduction pathways that regulate morphogenesis. Mucins can be classified into MUC1-20, which each have characteristic tandem repeat sequences. The amino acid residues of mucin are rich in serine and threonine, so have the potential to be O-glycosylated, and sugar chains constitute up to 80% of their molecular weight (1). In addition, mucins influence many cellular processes including growth, differentiation, transformation, adhesion, invasion, and immune surveillance. According to their cellular localization, mucins are divided into two classes: membrane bound mucins and secreted mucins. The secreted mucins, which lack a transmembrane domain and are secreted into extracellular spaces, include MUC2, MUC5AC, MUC5B, MUC6, MUC7, MUC8, and MUC19. The expression of secreted mucins is restricted to secretory organs and cell types. The membrane bound mucins, which are type I membrane proteins, include MUC1, MUC3, MUC4, MUC12, MUC13, MUC15, MUC16, MUC17, and MUC20. The membrane bound mucins are also considered to act as sensors of the external environment. Alterations in the gene expression of mucins accompany the development of cancer and influence cellular growth, differentiation, transformation, adhesion, and invasion (2-14). For example, aberrant expression of MUC4 in pancreatic, lung, breast, colon, and ovarian malignancies potentiates tumor cell growth and metastasis by altering the behavioral properties of tumor cells (15). MUC2-deficient mice showed increased proliferation, decreased apoptosis, and increased intestinal epithelial cell infiltration and frequently developed small intestinal, rectal, and gastrointestinal tumors (16). These results showed that MUC2 is involved in the suppression of cancer that protect the gastrointestinal tract.

It has been reported that MUC5AC is aberrantly expressed in premalignant and malignant lesions as well as in several pancreatic cancer cell lines, but is undetectable in normal pancreatic tissue (17-21; Ho *et al*, Gastroenterology 118: abs. 664, 2000). In our previous study, MUC5AC was expressed in 89.6% (60 of 67 cases) of pancreatic cancer cases (unpublished data). However, the details of how MUC5AC is involved in the process of malignant transformation, proliferation, and metastasis in pancreatic cancer remain to be elucidated. In the present study, we adapted the small interfering RNA (siRNA) technique to suppress MUC5AC expression in human pancreatic cancer cells and evaluated the effect of MUC5AC-knockdown on human pancreatic cancer cells *in vitro* and *in vivo* to clarify its functional role in human pancreatic cancer progression.

Materials and methods

Materials. The human pancreatic cancer cell lines SW1990, BxPC3, and PK-45P were purchased from Summit Pharmaceuticals International Corp. (Tokyo, Japan), Dainippon Sumitomo Pharma Biomedical Co. Ltd. (Osaka, Japan), and Cell Resource Center for Biomedical Research, Institute of Development, Aging and Cancer Tohoku University (Miyagi, Japan), respectively. The mouse anti-human MUC5AC monoclonal antibody (K-MAC5, IgG1) was developed in our laboratory. The rat anti-mouse CD45R/B220 monoclonal antibody (clone RA3-6B2) against B lymphocytes and the Ly-6G and Ly-6C (Gr-1, clone RB6-8C5) monoclonal antibody against granulocytes were purchased from Becton-Dickinson (San Jose, CA).

Mice. The experimental protocol was approved by the Ethics Committee on Animal Experiments of the Biomedical Research Laboratories of Kureha Corp., and the mice were treated in accordance with the guidelines of the committee. Five-week-old specific-pathogen-free female BALB/c-nu/nu mice purchased from Charles River Japan, Inc. (Kanagawa, Japan) were acclimatized for one week and then used in the experiments at the age of six weeks. The mice were allowed free access to sterilized CE-2 food (Oriental Yeast, Tokyo, Japan) and sterilized tap water and were bred at 25±2˚C, a humidity of 55±7%, laminar flow, and under a 12-h light/12-h dark cycle at 150-300 lux. To maintain a uniform environment, noise was carefully avoided, and only the experimenters and keepers were allowed into the animal room.

Cell culture conditions. SW1990 cells were cultured in Dulbecco's modified Eagle's medium (DMEM; Invitrogen Corp., San Diego, CA) supplemented with 10% fetal bovine serum (FBS; Biowest, Nuaill, France), 50 IU/ml penicillin, and 50 μg/ml streptomycin. BxPC3 and PK-45P cells were cultured in Roswell Park Memorial Institute (RPMI)-1640 (Invitrogen) supplemented with 10% FBS (Biowest), 50 IU/ml penicillin, and 50 μg/ml streptomycin. The cells were grown at 37˚C under 5% CO_2 in a humidified atmosphere and passaged before they reached confluency using 0.25% (w/v) trypsin solution containing 0.04% (w/v) EDTA.

Construction of the siRNA expression vector. Eight types of siRNA sequences (19-mer) against human MUC5AC were designed using a computer algorithm and tested for silencing efficacy in transient assays. The MUC5AC siRNA target sequence 5'-TTTGAGAGACGAAGGATAC-3' was found to be the sequence showing the most marked effects and cloned in order to generate a stable siRNA expressing construct into the p*Silencer* 3.1-H1 neo vector (Ambion, Inc., Austin, TX). Briefly, oligonucleotides (64-mer) encoding 19-mer hairpin sequences specific to the mRNA target were designed. These contained two complementary domains (sense and antisense) separated by the loop sequence 5'-TTCAAGAGA-3'. Double-stranded oligonucleotides were ligated into the p*Silencer* 3.1-H1 neo vector at *Bam*HI (Takara Bio Inc., Shiga, Japan) and *Hin*dIII (TaKaRa) restriction sites (p*Silencer*/si-MUC5AC). The plasmid was then amplified in chemically competent *Escherichia coli* (DH5α cells).

Quantitative real-time PCR. Quantitative real-time PCR (qRT-PCR) was performed with a Light Cycler system (Roche Diagnostics K.K., Tokyo, Japan) using the Light Cycler DNA master SYBR-Green I kit (Roche Diagnostics K.K.) according to the manufacturer's protocol. The following primers were used: for human MUC5AC gene: 5'-GCCACCGCTGCGGC CTTCTTC-3' (forward) and 5'-GTGCACGTAGGAGGACA GCGC-3' (reverse) and for human *glyceraldehyde-3-phosphate dehydrogenase (GAPDH)* gene: 5'-GAAGGTGAAGGTCGG AGTC-3' (forward) and 5'-GAAGATGGTGATGGGAT TTC-3' (reverse). *GAPDH* gene expression was used for cDNA normalization. Amplification was carried out as follows: initial denaturation at 95˚C for 15 min, followed by 40 cycles at 95˚C for 10 sec, a touchdown annealing (0.5˚C/cycle) from 68-60˚C for 10 sec, and elongation at 72˚C for 10 sec. After the completion of PCR amplification, a melting curve analysis was performed.

Transfection and selection of clones. SW1990 and BxPC3 cells were transfected with pSilencer/si-MUC5AC as a target vector or p*Silencer*/si-mock as a control vector using Genejuice (Merck, Darmstadt, Germany) according to the manufacturer's instructions. Briefly, the cells were seeded in a 100-mm culture dish and grown to 60-80% confluence. The medium was then removed, and the cells were washed twice in serum-free medium, before being incubated for 8 h in 15 ml serum-free medium with 18 μl Genejuice and 6 μg plasmid DNA. The cells were then washed in medium and cultured for 24 h in complete medium, and each cell was subcultured after 48 h (~5-fold). SW1990 and BxPC3 cells were selected by culturing them in the presence of geneticin at 600 and 400 μg/ml, respectively. The efficiency of MUC5AC-knockdown was tested by qRT-PCR and FACS analysis.

Fluorescence-activated cell sorting (FACS) analysis. The cells were detached using 0.04% (w/v) EDTA, washed with PBS, and resuspended in PBS containing 2% FBS and 2 mM EDTA (FACS buffer) and then were incubated with an appropriate dilution of K-MAC5 (1 μg), mouse serum (100-fold dilution), or isotype control (1 μg) per 10^6 cells for 2 h at 4˚C. After being washed three times in FACS buffer, the cells were incubated with a FITC-conjugated rabbit anti-mouse secondary antibody (Becton-Dickinson) for 30 min at 4˚C. The cells were then washed three times and resuspended

in FACS buffer, before being analyzed on a FACScan (Becton-Dickinson) with $>10^4$ cells analyzed per sample. The data files were analyzed using CellQuest (Becton-Dickinson), and the cells were gated using forward and side scatter variables to eliminate dead cells and debris.

Cell proliferation assay. The cells were suspended in each medium at a density of $1x10^4$/ml, and 100 μl suspensions were seeded in 96-well plates. After incubation for 0, 1, 2, 3, or 4 days, 20 μl of 3-(4,5-dimethylthiazol-2-yl)-2,5-diphenyltetrazolium bromide (MTT) solution (5 mg/ml) was added. Following incubation at 37˚C for 3 h, the supernatant was removed, and dimethylsulfoxide (DMSO) was added at 100 μl/well. The absorbance of formazan was measured at a wavelength of 570 nm and a reference wavelength of 630 nm with a Bio-Rad Microplate Reader 550 (Bio-Rad Laboratories Inc. Tokyo, Japan). Cell growth curves were plotted from the mean ± standard deviation (SD).

Tumorigenicity assay in xenograft models. Exponentially growing cells were detached with 0.25% (w/v) trypsin solution containing 0.04% (w/v) EDTA and resuspended in PBS at a density of $1x10^8$/ml. Each cell line ($1x10^7$/mice) was implanted s.c. into the flanks of nude mice, and their body weight and tumor volume were measured at least once a week. To determine tumor volume, two bisecting diameters were measured using a slide caliper, and the tumor volumes were calculated using the following formula: tumor volume = length x $(\text{width})^2$ x 0.5236 (22). At the end of the experiment, the tumors were removed, weighed, and fixed in 10% formaldehyde neutral buffer solution. Ten mice were used for each cell line. Tumors growth curves were plotted as the mean volume ± standard error (SE).

Metastasis assay. The experimental lung colonization was evaluated by injecting $1x10^6$ viable cells in 100 μl of PBS i.v. into the lateral tail vein of the BALB/c-nu/nu mice. The mice were euthanized on day 30 posttransplantation, their lungs were removed, and the total number of surface colonies was estimated under a dissecting microscope. Ten mice were used for each cell line.

Histology and immunohistochemistry. Lymphocyte infiltration into tumor tissue was evaluated by immunohistochemical analysis. Tumor tissues fixed in 10% formaldehyde neutral buffer solution were embedded in paraffin. Paraffin-embedded sections of 4 μm thickness were deparaffinized with xylene and ethanol, treated with 3% hydrogen peroxide solution for 20 min to inactivate endogenous peroxidase, and blocked with 2% porcine plasma in TBS for 15 min to reduce non-specific binding. Then, K-MAC5 monoclonal antibody, rat anti-mouse CD45R/B220 and Gr-1 monoclonal antibodies were added, and the sections were incubated at room temperature for 1 h. After being washed three times with TBS containing 0.05% Tween-20 (TBS-T), a horseradish peroxidase-labeled secondary antibody was added, and the sections were incubated at room temperature for 30 min. After being washed a further three times with TBS-T, immunoreaction was visualized with Liquid DAB Chromogen (Dako Japan Co. Ltd., Kyoto, Japan), and the sections were counterstained with hematoxylin. After being mounted on a glass slide with Entellan Neu (Merck), the stained specimens were examined using a microscope. In parallel to the immunostaining, hematoxylin and eosin (H&E) staining was performed for morphological evaluation.

Secondary tumor challenge. The primary tumor (SW1990/si-MUC5AC cells) was implanted via the injection of $1x10^7$ cells into the right flanks of nude mice. After 42 days, a secondary tumor (SW1990/si-mock cells) was implanted on the opposite flank. Tumor growth was measured at least once a week according to the above method.

Statistical analysis. All data are expressed as means ± SD or SE. Statistical significance was determined by the Student's t-test. P-values <0.05 were considered significant.

Results

Establishment of MUC5AC-knockdown cells by siRNA. The MUC5AC-overexpressed human pancreatic cancer cell lines SW1990 and BxPC3 were transfected with the p*Silencer* 3.1-H1 neo/si-MUC5AC vector or the p*Silencer* 3.1-H1 neo/si-mock vector as a negative control, and stable transfectants were established. In order to confirm the silencing efficiency of MUC5AC siRNA, the MUC5AC mRNA and protein levels in the transfectants were determined by qRT-PCR and FACS analysis. qRT-PCR data showed that MUC5AC expression was significantly decreased in stably transfected cells containing MUC5AC siRNA (SW1990/si-MUC5AC and BxPC3/si-MUC5AC cells) compared with si-mock cells containing the control vector (SW1990/si-mock and BxPC3/si-mock cells) (Fig. 1A). The loss of MUC5AC from the cell surface was determined by FACS analysis. It was found that the surface expression of MUC5AC was also substantially down-regulated in SW1990/si-MUC5AC and BxPC3/si-MUC5AC cells (si-MUC5AC transfectants) compared with the SW1990/si-mock and BxPC3/si-mock cells (si-mock transfectants), respectively (Fig. 1B). However, there were no differences between the si-mock transfectants and parental cells with regard to their mRNA and protein expression levels (data not shown). Therefore, in the following experiments, SW1990/si-mock and BxPC3/si-mock cells were used as negative controls.

In vitro cell survival, proliferation, and morphology. To investigate the effect of MUC5AC on cell proliferation, SW1990/si-mock, SW1990/si-MUC5AC, BxPC3/si-mock, and BxPC3/si-MUC5AC cells were seeded in 96-well plates and the number of cells was determined over time. As shown in Fig. 2A and B, no difference in cell proliferation was observed between the SW1990/si-MUC5AC and SW1990/si-mock cells or between the BxPC3/si-MUC5AC and BxPC3/si-mock cells. Next, we examined whether the knockdown of MUC5AC was associated with any morphological changes. Each cell was plated, and morphological changes were assessed during proliferation from sparsity to confluence. As a result, the SW1990/si-MUC5AC and BxPC3/si-MUC5AC cells tended to cluster together, and some of them exhibited a fibroblast-like morphology and a tightly packed cobblestone-like morphology, respectively (Fig. 2C), but the difference in

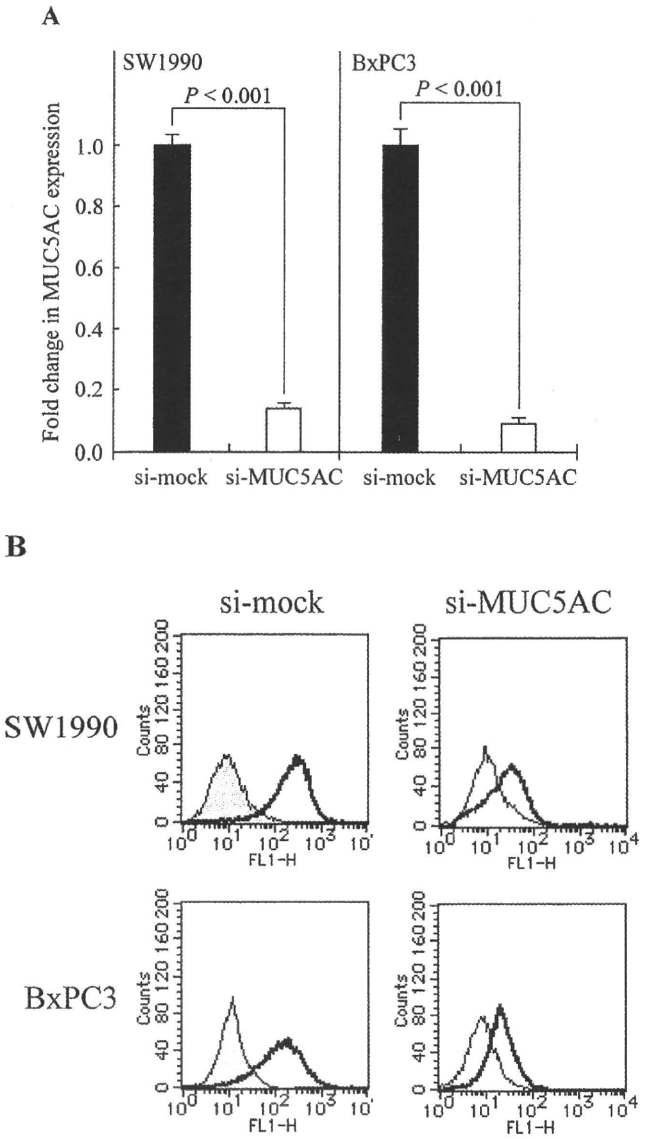

Figure 1. Establishment of MUC5AC-knockdown human pancreatic cancer cell lines. SW1990 and BxPC3 cells were stably transfected with p*Silencer* 3.1-H1 neo/si-mock or p*Silencer* 3.1-H1 neo/si-MUC5AC (an MUC5AC specific siRNA expression vector). The MUC5AC expression of each cell was then analyzed by qRT-PCR and FACS as described in Materials and methods. (A) MUC5AC and GAPDH mRNA expression levels were evaluated by qRT-PCR. qRT-PCR was performed on cDNA from each cultured cells using human MUC5AC-specific primers. Values were normalized using the internal control gene, *GAPDH*. All PCR experiments were performed in triplicate. Columns, mean of triplicate determinations; bars, SD. (B) FACS analysis of MUC5AC expression in mock- and MUC5AC-knockdown cells. Fluorescence of MUC5AC expressing SW1990 and BxPC3 cells probed with K-MAC5 mAb. Top, SW1990/si-mock and SW1990/si-MUC5AC cells; bottom, BxPC3/si-mock and BxPC3/si-MUC5AC cells; gray filled histograms, isotypic control antibody; bold lines, K-MAC5. The experiment was repeated twice. Representative data are shown.

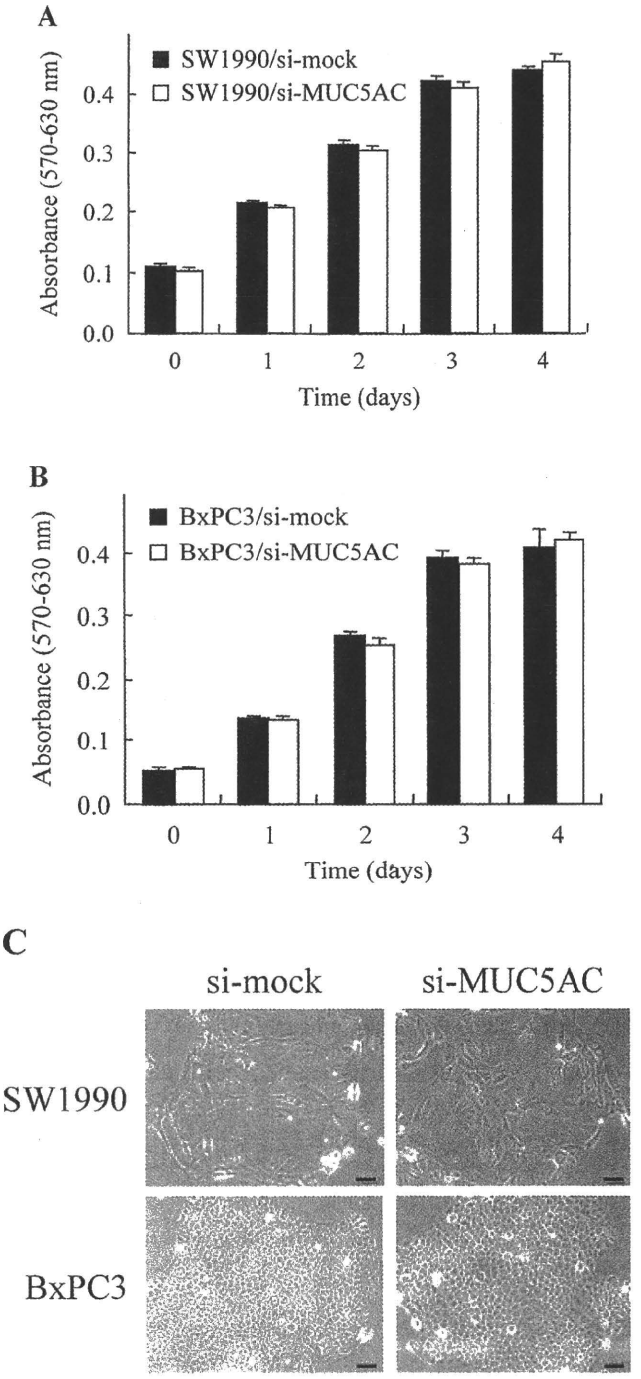

Figure 2. Effect of MUC5AC on cell growth and morphologic change. SW1990/si-mock and SW1990/si-MUC5AC (A) or BxPC3/si-mock and BxPC3/si-MUC5AC cells (B) seeded in a 96-well plate were cultured for 0, 1, 2, 3, or 4 days. Filled columns, si-mock cells; open columns, si-MUC5AC cells. Their cell number was determined by their absorbance as described in Materials and methods. The experiment was repeated thrice. Representative data are shown. Columns, mean of triplicate determinations; bars, SD. SW1990/si-mock and SW1990/si-MUC5AC (C, top) or BxPC3/si-mock and BxPC3/si-MUC5AC cells (C, bottom) were cultured during proliferation from sparsity to confluence, and phase-contrast microscopic images were observed. The experiment was repeated thrice. Data shown are representative images captured from one of three independent experiments performed in triplicate. Bar, 50 μm.

morphology between the si-mock and si-MUC5AC cells was not marked.

In vivo tumorigenicity and metastatic potential. As both the si-mock and si-MUC5AC cells showed exactly the same proliferation rate *in vitro*, we examined their ability to induce tumorigenicity *in vivo*. SW1990/si-MUC5AC cell-challenged mice barely developed any visible solid tumors, but the si-mock cell-challenged mice had developed tumors by one week as expected (Fig. 3A). The tumor growth of the SW1990/si-MUC5AC cells was suppressed compared to that of the

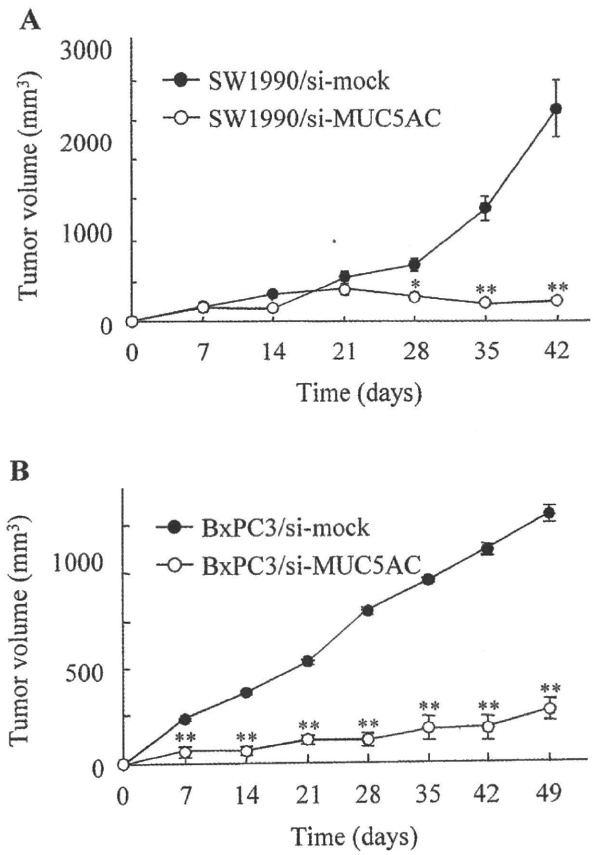

Figure 3. MUC5AC-knockdown by siRNA significantly inhibited tumor xenograft growth. (A) Tumor growth curves of SW1990/si-mock (filled circles) and SW1990/si-MUC5AC (open circles) cells. (B) Tumor growth curves of BxPC3/si-mock (filled circles) and BxPC3/si-MUC5AC (open circles) cells. The cells were s.c. implanted with $1x10^7$ cells into the nude mice on day 0. The mice were monitored for tumor formation until 42 (A) and 49 (B) days, respectively, and the tumors were measured on the indicated days. These experiments were repeated at least thrice. Representative data are shown. Points, mean tumor volume of 10 mice for each group; bars, SE. Statistically significant at $^*P<0.005$ and $^{**}P<0.001$ (versus si-mock cell-challenged mice group).

SW1990/si-mock cells after day 28 ($P<0.005$). Also tumor volumes were significantly increased in the mice injected with BxPC3/si-mock cells compared with the tumor growth in those injected with BxPC3/si-MUC5AC cells (Fig. 3B). The tumor growth of the BxPC3/si-MUC5AC cells was decreased compared with that of the BxPC3/si-mock cells after day 7 ($P<0.001$). Furthermore, to examine whether the proliferation of si-MUC5AC cells was also inhibited in a lung metastasis model, the SW1990/si-mock and SW1990/si-MUC5AC cells were injected i.v. into nude mice, and metastases were enumerated after day 30. As a result, there were no lung metastases that could be confirmed under a dissecting microscope in the SW1990/si-MUC5AC cell-challenged mice, while many metastases were observed in the SW1990/si-mock cell-challenged mice (Table I).

Accumulation of immunocytes in the tumor tissues. To identify the types of immunocytes that infiltrated into the tumor tissues, the tumor challenge sites were removed and subjected to histological and immunohistochemical examination. First, MUC5AC expression at the SW1990/si-mock cell-challenged site and SW1990/si-MUC5AC cell-challenged site was examined by IHC using K-MAC5 monoclonal antibody, and its significant suppression at the latter site was confirmed (Fig. 4A). Next, rat anti-mouse CD45R/B220 and Gr-1 monoclonal antibodies were used for the detection of the B lymphocytes and granulocytes, respectively. As shown in Fig. 4B, H&E staining showed that many immunocytes had infiltrated into the SW1990/si-MUC5AC cell-challenged site. Immunohistochemistry revealed that the infiltrating cells were CD45R/B220$^+$ (Fig. 4C) and Gr-1$^+$ cells (Fig. 4D) that were scattered throughout the tumor, but were particularly localized in the epithelial and surrounding stromal compartments. In contrast, few or no infiltrating immunocytes were found at the SW1990/si-mock cell-challenged site.

Table I. MUC5AC-knockdown in tumor cells significantly diminishes lung metastasis.[a]

	Count of lung metastases									
Mice no.	1	2	3	4	5	6	7	8	9	10
SW1990/si-mock	4	10	3	5	6	8	7	6	10	4
SW1990/si-MUC5AC	0	0	0	0	0	0	0	0	0	0

[a]Tumor cells ($1x10^6$) were injected into the lateral tail veins of the mice. The lungs were collected 30 days after posttransplantation, and the total numbers of surface colonies were counted. Ten mice were used for each cell line. The experiment was repeated twice. Representative data are shown.

Antibody production by B lymphocytes. As it was shown in the above immunostaining examination that many B lymphocytes had accumulated at the SW1990/si-MUC5AC cell-challenged site, we investigated whether B lymphocytes raised specific antibodies against the implanted tumor cells. To do this, sera were collected from SW1990/si-mock and SW1990/si-MUC5AC cell-challenged mice and were used to evaluate the responsiveness to human pancreatic PK-45P cells, which do not express MUC5AC, by FACS analysis. FACS analysis showed that the sera of the SW1990/si-MUC5AC cell-challenged mice more effectively recognized PK-45P cells as a foreign substance, compared to that of the SW1990/si-mock cell-challenged mice (Fig. 4E).

Rejection of a secondary challenge with SW1990/si-mock cells in mice subjected to primary challenge with SW1990/si-MUC5AC cells. It was thought that memory B cells may play a pivotal role in the rejection of grafted SW1990/si-MUC5AC cells in nude mice. So, we investigated whether a secondary challenge with SW1990/si-mock cells would be rejected in mice that had previously been challenged with SW1990/si-MUC5AC cells. As a first step, SW1990/si-MUC5AC cells (the primary tumor) were implanted into the right flanks of nude mice. After 42 days, SW1990/si-mock cells

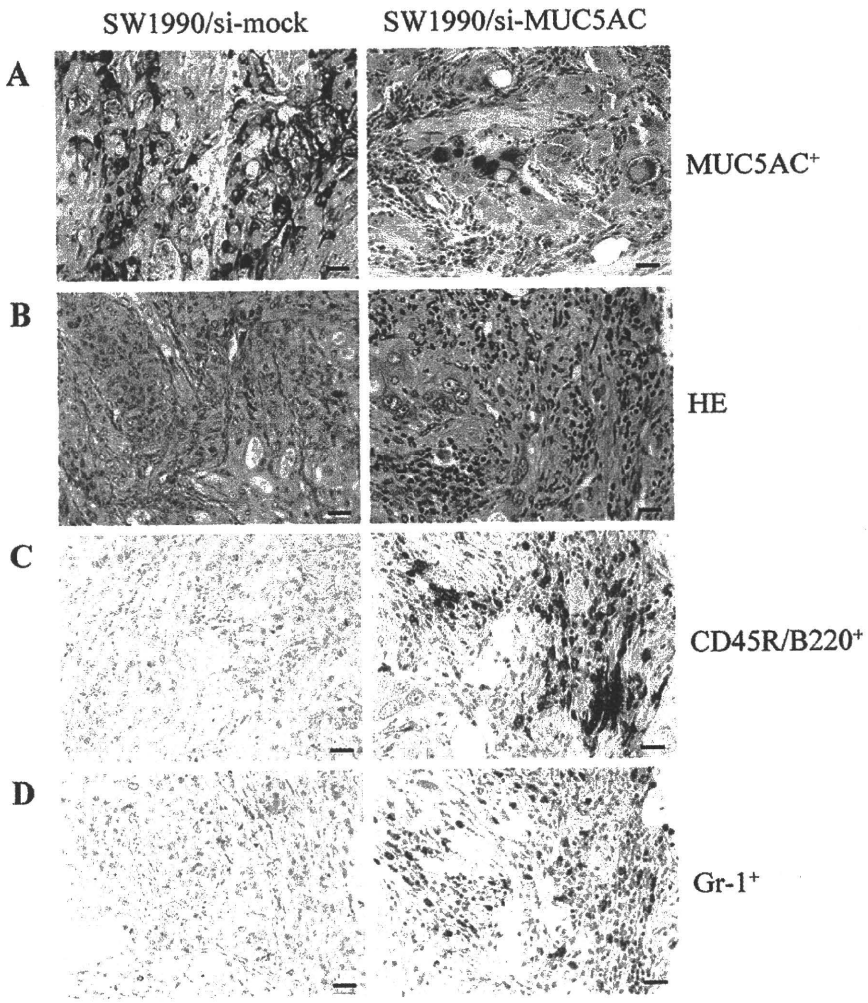

Figure 4. MUC5AC inhibits the accumulation of immunocytes into tumor tissue. The tumors challenged in the experiment shown in Fig. 3A were subjected to histological and immunohistochemical examinations. Tumor sections obtained from SW1990/si-mock (left) and SW1990/si-MUC5AC (right) cell-challenged mice were treated with mouse anti-human MUC5AC monoclonal antibody (A), H&E (B), rat anti-mouse CD45R/B220 (C), and Gr-1 (D) monoclonal antibodies as described in Materials and methods. Representative stainings are shown. Bar, 20 μm. (E) MUC5AC suppresses antibody production against implanted tumor cells. Serum was collected from each of the SW1990/si-mock and SW1990/si-MUC5AC cell-challenged mice in the experiment shown in Fig. 3A, and equivalent amounts of each serum (n=10) were mixed and diluted to 1:100. The mixed serum was used to evaluate the responsiveness to PK-45P cells by FACS analysis as described in Materials and methods. Gray filled histogram, normal control serum; thin line, the mixed serum from SW1990/si-mock cell-challenged mice; bold line, the mixed serum from SW1990/si-MUC5AC cell-challenged mice. All these experiments were performed at least thrice. One representative data set of three independent experiments is shown.

(the secondary tumor) were implanted into the opposite flank (Fig. 5A). As a result, the secondary tumor growth of SW1990/si-mock cells was significantly decreased in the primary tumor-bearing mice compared with the primary tumor-absent mice (Fig. 5B). Significant inhibition was shown after day 7 of the secondary challenge ($P<0.001$). In other words, the primary graft of SW1990/si-MUC5AC cells caused strong rejection of the secondary tumor graft. Furthermore, the primary tumor no longer developed and was not promoted by the secondary inoculation (data not shown). In contrast, the tumor volumes of the SW1990/si-mock cells in the primary tumor-absent mice were significantly increased, as expected from the results shown in Fig. 3A.

Discussion

In spite of recent developments that have improved the prevention, screening, and therapy for pancreatic cancer, it still has a poor prognosis: a 5-year survival rate of up to 3% and a median survival of up to 6-month. This poor prognosis

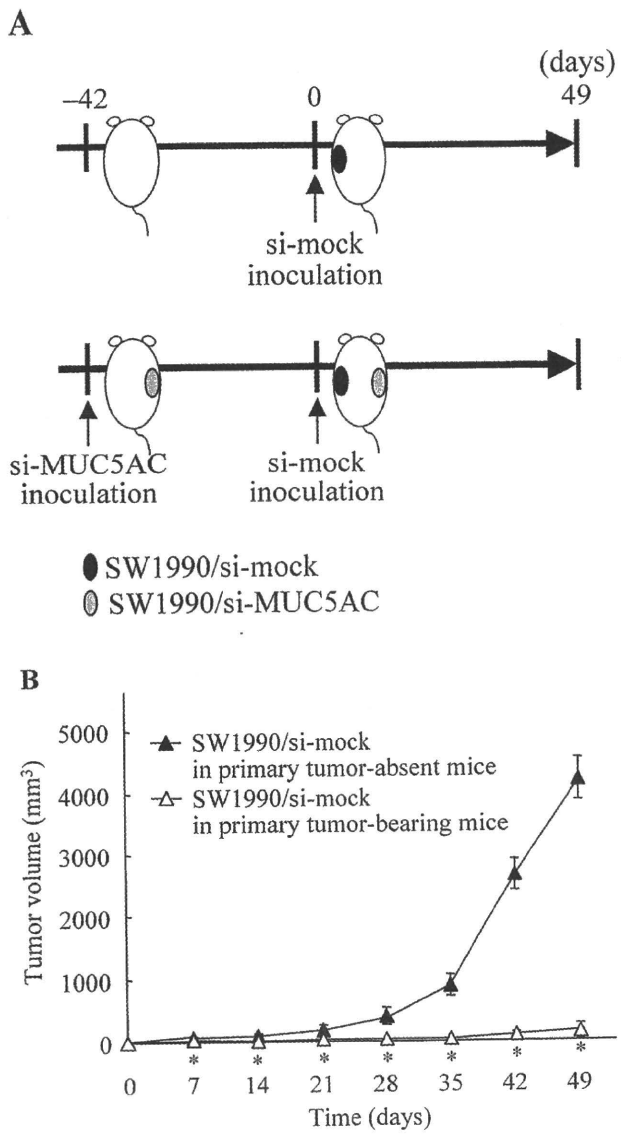

Figure 5. MUC5AC suppresses the immune memory system. (A) Animal experiment protocol. (B) Tumor volume. The primary tumor (SW1990/si-MUC5AC cells) was implanted with $1x10^7$ cells into the flanks of nude mice. After 42 days, a secondary tumor (SW1990/si-mock cells) was implanted with $1x10^7$ cells into the primary tumor-absent mice (filled triangles) and the primary tumor-bearing mice (open triangles). Tumor size was measured on the indicated days. These experiments were repeated at least thrice. Representative data are shown. Points, mean tumor volume of 10 mice for each group; bars, SE. Statistically significant at $^*P<0.001$ (versus primary tumor-absent mice group).

is a consequence of metastatic disease, which results from a lack of early detection and effective treatment. Concerning the relationship between the malignancy grade of pancreatic cancer and mucins, it was previously reported that MUC1 and carbohydrate antigens such as sialyl Lewis antigen are related to metastatic potential and prognosis. For example, Tsutsumida *et al* previously reported that down-regulation of MUC1 expression by siRNA significantly decreased human pancreatic cancer cell proliferation *in vitro* and *in vivo* (23). Chaturvedi *et al* demonstrated that silencing MUC4 expression by transfecting MUC4-specific short hairpin RNA into a human pancreatic cell line decreased cell growth and metastasis *in vivo* and induced ectopic expression of growth- and metastasis-associated genes. They also showed that over-expression of MUC4 is associated with increased tumor cell growth and metastasis via interference with the interaction between cancer cells and extracellular matrix proteins (24).

MUC5AC has been shown to be a major component of the stomach and airway, and little or no expression of MUC5AC is found in other normal tissues; whereas, it is anomalously expressed in human pancreatic and colorectal cancers. This implies that MUC5AC plays an important role in these cancers, but few reports exist on its function. Here, we established MUC5AC-knockdown cells by introducing siRNA and investigated how MUC5AC contributes to tumor progression. The findings from the present study showed that the ectopic expression of MUC5AC was not involved in cell growth *in vitro*, but that it was intimately involved in tumor growth *in vivo*. The expression levels of cell-adhesion factors, some of which, such as sialyl-Lewis^a, sialyl-Lewis^x, and E-cadherin are known to be related to metastasis, were not affected in si-MUC5AC cells (data not shown). In addition, to test the alteration in migratory capacity after the suppression of MUC5AC, we performed a scratch wound-healing assay in si-MUC5AC and si-mock cells. The scratch wound-healing assay is considered to be an *in vitro* model of the epithelial cell migration that occurs during wound healing. The scratch wounds in both cells were closed with a large portion after 48 h and no significant delay in the migration of si-MUC5AC cells into the empty space was observed (data not shown). Therefore, it appears that the functions of MUC5AC in pancreatic cancer are essentially different from those of other mucins. In the future, we are going to perform a microarray analysis of si-mock and si-MUC5AC cells and to investigate the expression of tumor-associated genes.

An analysis of the functional role of MUC5AC was reported for colorectal cancer. It may be assumed that the expression of MUC5A plays a role in the invasiveness of cancers, as it is detected in the early stages of human colorectal cancer. Truant *et al* reported on the invasive properties of the human colon carcinoma cell line HT-29 (HT-29 STD) and its highly MUC5AC secreting-variant (HT-29 5M21). It was found that HT-29 STD cells are non-invasive; whereas, HT-29 5M21 cells are invasive due to a lack of cell-cell adhesion through E-cadherin, and HT-29 STD cells and HT-29 5M21 cells also have different morphologies, the former grows in multilayers, but the latter grows in monolayers (25). In the present study, MUC5AC-knockdown cells and their parental cells proliferated in multilayers and did not differ in morphology (Fig. 2). These results indicate that the MUC5AC molecules of pancreatic and colorectal cancers may have different functions.

In a previous report, mucins were found to have inhibitory effects on the antitumor response of the host and to promote tumor progression and metastasis. Cell-cell adhesion contributes to the normal development and function of cells; whereas, the highly glycosylated rigid structure of the mucins reduces both homotypic cell-cell adhesion and cell-substratum interactions (26). Almost all of the functions of mucins reported until now have been connected to proliferation, adhesion, migration, or invasion, and *in vitro* as well as *in vivo* proliferation has been reported to be inhibited by knockdown

of the expression of mucins. However, the present study demonstrated that MUC5AC-knockdown affected *in vivo* proliferation but not *in vitro* proliferation, which differs from the results of previous reports. As shown in Figs. 2 and 3, MUC5AC-knockdown cells showed similar results to the control cells with regard to cell survival, proliferation, and morphology *in vitro*. However, in *in vivo* xenograft studies, their tumor growth was significantly inhibited compared with that of the control cells. So, why were *in vivo* tumorigenicity and metastasis inhibited when no marked *in vitro* effect was observed? One of the reasons for this inhibitory effect is thought to be induced by antibody-dependent cell-mediated cytotoxicity (ADCC). In the present study, B cells and neutrophils were found to accumulate at SW1990/si-MUC5AC cell-challenged sites (Fig. 4). Moreover, a greater number of antibodies against human pancreatic cells were present in the blood of the SW1990/si-MUC5AC cell-challenged mice compared to the levels produced by the SW1990/si-mock cell-challenged mice (Fig. 4E). Neutrophils are non-specific cytotoxic immunocytes that exclude infecting organisms. Recently, it has been reported that neutrophils also have antitumor effects mediated through ADCC via phagocytosis, elastase, or superoxide (27-29). ADCC is triggered by tumor-specific antibodies and Fc receptor-expressing cytolytic cells such as NK cells, neutrophils, eosinophils, and monocytes/macrophages (30). According to these results, the present *in vivo* tumor inhibition was supposed to be induced by ADCC. Moreover, si-MUC5AC cells are a MUC5AC-knockdown cell line and are not able to grow *in vivo*. The SW1990/si-MUC5AC cell-challenged mice used in this study significantly rejected a secondary tumor challenge with SW1990/si-mock cells, which are usually able to grow *in vivo* (Fig. 5B). As nude mice were used in the present experiments, antigen memory via cytotoxic T cells can not be involved. Therefore, the mice that received the si-MUC5AC cells might have produced specific antibodies against an unknown pancreatic cancer specific antigen, and these antibodies may have inhibited the secondary-challenged si-mock tumor via ADCC. It would be interesting to know which molecule serves as the antigen in this case, as its identification and analysis would provide a target for molecular pancreatic cancer therapeutics.

Another possible reason for the *in vivo* inhibition of tumorigenicity is that MUC5AC is directly involved in immune suppression and avoidance. Several reports have investigated MUC1 or MUC2. Overexpression of MUC1 in pancreatic cancer is associated with poor prognosis (31), and there is disputed evidence that tumors associated with MUC1 directly influence the response of immunocytes. For example, MUC1 inhibits the function of effector cells such as natural killer cells, lymphokine-activated killer cells, and cytotoxic T-cells. Also, soluble MUC1 induces apoptosis of activated T cells and inhibits the proliferation of natural killer cells and cytotoxic T-cells (32,33). MUC2 has been reported to bind to a scavenger receptor of monocytes/macrophages and leads to the overproduction of PGE2, which suppresses immunocytes through COX2 (34,35). In this study, the growth of MUC5AC-knockdown cells was inhibited in not only xenografted tumors but also a lung metastasis mode (Table I). Thus, it has been suggested that MUC5AC may be involved in immunosuppression and evasion from the immune system similarly to MUC1 and MUC2. However, future studies are needed to investigate the immunosuppressive mechanism of MUC5AC in human pancreatic cancer.

In conclusion, we investigated the role of MUC5AC in human pancreatic cancer progression using specific siRNA against MUC5AC. Our data showed that suppression of MUC5AC in two human pancreatic cancer cell lines dramatically reduced *in vivo* tumor growth and metastasis without affecting cell growth *in vitro*. Also infiltration of $CD45R/B220^+$ and $Gr\text{-}1^+$ cells was observed in tumor tissue generated by implanting si-MUC5AC cells into mice. Furthermore, specific antibodies against the tumor cells were mostly observed in the sera of SW1990/si-MUC5AC cell-bearing mice. These results suggested that the MUC5AC expressed on the surface of pancreatic cancer cells aids cancer cell escape from the immune system. The present findings highlight a new dimension of MUC5AC as a functional immunosuppressive agent and its important role in pancreatic cancer progression. Also, MUC5AC may be an important indicator for the diagnosis and prognosis of pancreatic cancer, and disruption of MUC5AC may have potential as a treatment for MUC5AC-expressing pancreatic and other cancers.

Acknowledgements

This work was conducted at Kureha Corporation, Tokyo, Japan and Osaka City University, Osaka, Japan. Hirotaka Hoshi, Motoyuki Uchida, Hikaru Saito, Hiroko Iijima, Mikako Toda-Agetsuma, and Tsutomu Wada are employees of Kureha Corporation, but the study was conducted with scientific integrity and presents no conflict of interest.

References

1. Carlstedt I, Sheehan JK, Corfield AP and Gallagher JT: Mucus glycoproteins: a gel of a problem. Essays Biochem 20: 40-76, 1985.
2. Bobek LA, Tsai H, Biesbrock AR and Levine MJ: Molecular cloning, sequence, and specificity of expression of the gene encoding the low molecular weight human salivary mucin (MUC7). J Biol Chem 268: 20563-20569, 1993.
3. Gum JR Jr, Hicks JW, Swallow DM, *et al*: Molecular cloning of cDNA derived from a novel human intestinal mucin gene. Biochem Biophys Res Commun 171: 407-415, 1990.
4. Gum JR Jr, Hicks JW, Toribara NW, Rothe EM, Lagace RE and Kim YS: The human MUC2 intestinal mucin has cysteine-rich subdomains located both upstream and downstream of its central repetitive region. J Biol Chem 267: 21375-21383, 1992.
5. Gum JR Jr, Hicks JW, Toribara NW, Siddiki B and Kim YS: Molecular cloning of human intestinal mucin (MUC2) cDNA. Identification of the amino terminus and overall sequence similarity to prepro-von Willebrand factor. J Biol Chem 269: 2440-2446, 1994.
6. Gum JR Jr, Crawley SC, Hicks JW, Szymkowski DE and Kim YS: MUC17, a novel membrane-tethered mucin. Biochem Biophys Res Commun 291: 446-475, 2002.
7. Hollingsworth MA and Swanson BJ: Mucins in cancer: protection and control of the cell surface. Nat Rev Cancer 4: 45-60, 2004.
8. Moniaux N, Nollet S, Porchet N, Degand P, Laine A and Aubert JP: Complete sequence of the human mucin MUC4: a putative cell membrane-associated mucin. Biochem J 338: 325-333, 1999.
9. Fauquette V, Aubert S, Groux-Degroote S, Hemon B, Porchet N, van Seuningen I and Pigny P: Transcription factor AP-2 represses both the mucin MUC4 expression and pancreatic cancer cell proliferation. Carcinogenesis 28: 2305-2312, 2007.